

1 **Interactions of pathogenic and commensal strains of**
2 ***Mannheimia haemolytica* with differentiated bovine**
3 **airway epithelial cells grown at an air-liquid**
4 **interface**

5 **Daniel Cozens¹, Erin Sutherland¹, Miquel Lauder¹, Geraldine Taylor², Catherine C.**
6 **Berry³ and Robert L. Davies^{1*}.**

7

8 ¹ *Institute of Infection, Immunity and Inflammation, College of Medical, Veterinary and Life*
9 *Sciences, University of Glasgow, Glasgow, UK*

10 ² *The Pirbright Institute, Pirbright, Surrey, UK*

11 ³ *Institute of Molecular, Cell and Systems Biology, College of Medical, Veterinary and Life*
12 *Sciences, University of Glasgow, Glasgow, UK*

13

14

15 *Corresponding Author

16 Email: robert.davies@glasgow.ac.uk

17

18 **Abstract**

19 *Mannheimia haemolytica* serotype A2 is a common commensal species present in the
20 nasopharynx of healthy cattle. However, prior to the onset of bovine pneumonic
21 pasteurellosis, there is sudden increase in *M. haemolytica* serotype A1 within the upper
22 respiratory tract. The events during this selective proliferation of serotype A1 strains are
23 poorly characterised. In this investigation, a differentiated bovine airway epithelial cell
24 culture was used to study the interactions of A1 and A2 bovine isolates with the respiratory
25 epithelium. This model reproduced the key defences of the airway epithelium, including tight
26 junctions and mucociliary clearance. Although initial adherence of the serotype A1 strains
27 was low, by 12 hours post-infection the bacteria was able to traverse the tight junctions to
28 form foci of infection below the apical surface. The size, density and number of these foci
29 increased with time, as did the cytopathic effects observed in the bovine bronchial epithelial
30 cells. Penetration of *M. haemolytica* A1 into the sub-apical epithelium was shown to be
31 through transcytosis but not paracytosis. Commensal A2 bovine isolates however were not
32 capable of colonising the model to a high degree, and did not penetrate the epithelium
33 following initial adherence at the apical surface. This difference in their ability to colonise the
34 respiratory epithelium may account for the sudden proliferation of serotype A1 in the onset of
35 pneumonia pasteurellosis. The pathogenesis observed was replicated by virulent A2 ovine
36 isolates; however colonisation was 10-fold lower in comparison to bovine A1 strains. This
37 investigation provides new insight into the interactions of *M. haemolytica* with bovine airway
38 epithelial cells which are occurring *in vivo* during pneumonia pasteurellosis.

39 **Introduction**

40 Bovine respiratory disease (BRD) is a multifactorial condition of cattle that causes significant
41 economic losses (>\$3 billion annually in the USA alone) to the cattle industry worldwide [1-
42 3]. The pathogenesis of BRD is complex, involving poorly understood interactions between
43 various viral and bacterial pathogens and the host; environmental stress is also an important
44 pre-disposing factor leading to the outbreak of disease [3-6]. Although many of the viral and
45 bacterial pathogens can potentially cause disease themselves, it is generally accepted that
46 viral infection often occurs first and predispose cattle to subsequent bacterial infection [3-9].
47 Pneumonic pasteurellosis is one of the most severe forms of BRD; it is characterized by an
48 acute lobar fibronectinizing pneumonia or pleuropneumonia and is associated with the
49 bacterial pathogen *M. haemolytica* [3, 5, 10, 11].

50 *Mannheimia haemolytica* occurs naturally as a commensal in the upper respiratory tract of
51 healthy cattle [12, 13] but, under circumstances described above, is frequently associated
52 with disease [1, 10, 12]. The bacterium comprises 12 capsular serotypes [14] but it is widely
53 recognized that serotype A2 strains are most commonly associated with healthy cattle, where
54 they reside as commensals in the nasopharynx and tonsils; conversely, serotype A1 (and more
55 recently A6) strains are mainly responsible for disease [1, 3, 10, 15, 16]. However, in
56 addition to differences in capsular polysaccharide biochemistry and structure [17, 18],
57 serotype A1/A6 and A2 strains of *M. haemolytica* represent distinct chromosomal genotypes
58 [19, 20] and can also be distinguished by differences in their outer membrane protein (OMP)
59 profiles [21], lipopolysaccharide types [21, 22] and nucleotide sequence variation in various
60 virulence-associated genes including *lktA* [23], *ompA* [24], *tbpA* and *tbpB* [25], *plpE* [26] as
61 well as a number of other genes [20]. The upper respiratory tract of healthy cattle is
62 predominantly colonized by serotype A2 strains but, for reasons that are not clear (but
63 probably related to stress and/or viral infection), a transition occurs within this

64 microenvironment which leads to a sudden explosive proliferation in the number of serotype
65 A1/A6 bacteria present and subsequent colonization [1, 3]. This sudden and selective
66 explosion in the A1/A6 population within the upper respiratory tract leads to the inhalation of
67 bacteria-containing aerosol droplets into the trachea and lungs and the onset of pneumonic
68 pasteurellosis [27]. Crucially, the specific bacterial and host factors responsible for the
69 sudden shift from commensal serotype A2 to pathogenic serotype A1/A6 populations within
70 the upper respiratory tract are not clear.

71 The leukotoxin (LktA) of *M. haemolytica* plays a central role in the pathogenesis of
72 pneumonic pasteurellosis and significant attention has been given to understanding the
73 molecular mechanisms associated with LktA activity within the lung [1, 3, 28, 29]. In
74 contrast, there has been far less focus on the interactions of *M. haemolytica* with respiratory
75 airway epithelial cells and events that might account for the sudden proliferation of serotype
76 A1/A6 bacteria within the upper respiratory tract. A contributing factor to our poor
77 understanding of early host-pathogen interactions associated with pneumonic pasteurellosis,
78 and indeed BRD in general, is the lack of physiologically-relevant and reproducible
79 methodologies with which to study the intricate molecular and immunological interactions
80 between pathogens and host. Traditionally, submerged, two-dimensional cultures of a single
81 cell type have been used to investigate interactions of *M. haemolytic* and other BRD
82 pathogens within the bovine respiratory tract [30-32] but these have numerous limitations:
83 they do not reflect the multicellular complexity of the parental tissue *in vivo*, they lack its
84 three-dimensional (3-D) architecture, and the physiological conditions are not representative
85 of those found within the respiratory tract. However, these characteristics that are lacking in
86 submerged cultures can be recapitulated using differentiated airway epithelial cells (AECs)
87 grown at an air-liquid interface (ALI) and, in recent years, such cell culture approaches have

88 been used to study the interactions of various bacterial and viral pathogens with different host
89 species [33-43].

90 We have previously investigated the growth conditions required for optimal growth and
91 differentiation of bovine bronchial epithelial cells at an ALI [44] and assessed the temporal
92 differentiation of these cells to identify an optimum window suitable for infection studies
93 [45]. The aim of the present study was to investigate the interactions of a panel of *M.*
94 *haemolytica* isolates, representing virulent and commensal strains recovered from both cattle
95 and sheep, with differentiated bovine bronchial epithelial cells grown at an ALI. The course
96 of infection was followed for up to five days using various microscopic approaches and the
97 production of selected cytokines measured to ascertain the epithelial cell response.

98 **Materials and Methods**

99 **Bacterial cultures**

100 Eight wild-type *M. haemolytica* strains (Table 1) isolated from both cattle and sheep were
101 included in this investigation. The strains were isolated from either pneumonic or healthy
102 animals. Bacteria were routinely grown on brain-heart infusion (BHI) agar supplemented
103 with 5% (v/v) defibrinated sheep blood overnight at 37 °C. Broth cultures were grown in
104 BHI broth at 37 °C with agitation.

105 **Culture of bovine bronchial epithelial cells**

106 Bronchial epithelial cells were isolated from cattle aged 24-30 months, as described by
107 Cozens *et al.* Tissue was collected from cattle immediately post-slaughter at Sandyford
108 Abattoir Ltd., UK. The bronchial tract was swabbed to ensure there was no pre-existing
109 bacterial or fungal infection. *Ex vivo* bronchi tissue was also collected, fixed in 2% (w/v)
110 formaldehyde and sectioned for histological analysis to confirm the health of the donor

111 animal. Briefly, the main and lobar bronchi were dissected from the lungs and the
112 surrounding tissue removed. The BBECs were isolated from the epithelium by incubation
113 overnight at 4°C in ‘digestion medium’ composed of Dulbecco’s modified Eagle’s medium
114 (DMEM) and Ham’s nutrient F-12 (1:1) containing 1 mg/ml dithioereitol, 10 µg/ml DNAase
115 and 1 mg/ml Protease XIV from *Streptomyces griseus*, supplemented with penicillin (100
116 U/ml), streptomycin (100 µg/ml) and amphotericin (2.5 µg/ml) (Sigma-Aldrich). All
117 subsequent media, with the exception of media utilised during infection of the BBEC cultures
118 were also supplemented with penicillin-streptomycin and amphotericin. Digestion of the
119 bronchial epithelium was halted by the addition of foetal calf serum to give a final
120 concentration of 10% (v/v). Rigorous rinsing of the luminal surface was used to remove
121 loosely-attached epithelial cells. The resulting suspension was centrifuged and resuspended
122 in ‘submerged growth medium’ (SGM), comprised of DMEM/Ham’s F-12 (1:1)
123 supplemented with 10% (v/v) foetal calf serum. Cells were seeded into T75 tissue culture
124 flasks (5×10^6 cells/flask) for expansion. The flasks were incubated at 37°C in 5% CO₂ and
125 14% O₂, in a humidified atmosphere. At 80-90 % confluency (~4 days post-seeding) the
126 flasks of BBECs were harvested. Cells were detached using 0.25% trypsin-EDTA solution,
127 centrifuged and resuspended in SGM at a density of 5×10^5 cells/ml. The BBECs were
128 seeded into the apical chamber of tissue culture inserts (Thincerts, Greiner #66540,
129 polyethylene terephthalate membrane, 0.4 µm pore diameter, 1×10^8 pore per cm²) at a
130 density of 2.5×10^5 cells per insert. Cultures were incubated at 37 °C, 5% CO₂, 14% O₂, in a
131 humidified atmosphere. Following overnight incubation, the apical medium of the culture
132 was removed and the apical surface washed with 0.5 ml PBS to remove unattached cells. The
133 SGM media in the apical and basolateral compartments was then replaced. This process was
134 repeated every 2 – 3 days. The trans-epithelial electrical resistance (TEER) of the cultures
135 were monitored on a daily basis using an EVOM2 epithelial voltohmmeter (World Precision

136 Instruments, UK), as per the manufacturer's instruction. Once the TEER reached above 200
137 Ω/cm^2 (~2 days post-seeding) the SGM was replaced with a mixture of SGM and 'air-liquid
138 interface medium' (ALIM) (1:1). The ALIM was composed of DMEM and airway epithelial
139 cell growth medium (Promocell) (1:1) supplemented with 10 ng/ml epidermal growth factor,
140 100 nM retinoic acid, 6.7 ng/ml triiodothyronine, 5 $\mu\text{g}/\text{ml}$ insulin, 4 $\mu\text{l}/\text{ml}$ bovine pituitary
141 extract, 0.5 $\mu\text{g}/\text{ml}$ hydrocortisone, 0.5 $\mu\text{g}/\text{ml}$ epinephrine and 10 $\mu\text{g}/\text{ml}$ transferrin (all
142 Promocell). When the TEER value was above 500 $\Omega \text{ cm}^2$ (~6 days post-seeding), an ALI
143 was generated by removing the medium in the apical compartment, thereby exposing the
144 epithelial cells to the atmosphere (day 0 post-ALI). Following the formation of the ALI, the
145 cells were fed exclusively from the basal compartment with ALIM. Apical washing, basal
146 feeding and TEER measurements were performed every 2 - 3 days until day 21 post-ALI.

147 **Infection of bovine bronchial epithelial cells**

148 The BBEC cultures were infected on day 21 post-ALI. The apical and basal compartments
149 were washed twice with PBS, 24 hours prior to infection. The cultures were subsequently fed
150 with 1 ml ALIM with the omission of penicillin-streptomycin and amphotericin. Bacteria
151 used in the infection were collected from fresh overnight plate cultures, grown in BHI broth
152 to exponential phase, and resuspended in PBS at 10^9 cfu/ml. The bacterial suspension was
153 used to inoculate the BBEC cultures apically. Each insert was inoculated with 25 μl of
154 bacterial suspension (2.5×10^7 cfu/insert). Cultures were incubated at 37 °C until the stated
155 time point post-infection. For infection of undifferentiated BBECs, cultures were infected at
156 day 0 post-ALI.

157 **Quantification of bacterial adhesion**

158 At stated time points following infection, a viability count was performed on the adherent *M.*
159 *haemolytica*. The ALIM was removed from the basal compartment and the apical surface of
160 the transwell was washed three times with 1 ml PBS. The three washes were subsequently

161 pooled and the number of viable bacteria was also assessed. The BBEC were incubated in
162 0.5 ml PBS with 1% Triton X-100 to permeabilise the epithelial cells. The membrane was
163 scraped to mechanically disintegrate the culture. Viable bacteria in the lysate and apical
164 washes were quantified using 10-fold serial dilutions, performed in triplicate, and plating on
165 BHI agar with 5% (v/v) defibrinated sheep blood, using the Miles and Misra method. Plates
166 were incubated for six hours at 37 °C and the number of colony-forming units (CFU)
167 counted. Bacterial number was expressed as a percentage of the inoculum. For the
168 gentamicin protection assay, the apical surface was treated with 200 µg/ml gentamicin for
169 one hour at 37 °C prior to permeabilisation. For each animal, bacterial adherence was
170 quantified in three independent BBEC cultures at all time points.

171 **Histology and immunohistochemistry**

172 At the stated time points post-infection, cultures were fixed by incubation with 4% (w/v)
173 paraformaldehyde for 15 min at room temperature and rinsed in PBS. The samples were
174 subsequently dehydrated using a series of increasing ethanol concentrations, cleared with
175 xylene and infiltrated with paraffin wax. Sections of the wax blocks were cut at 2.5 µm
176 thickness using a ThermoShandon Finesse ME+ microtome. Samples were stained with
177 haematoxylin and eosin (H&E) using standard histological techniques. Further sections were
178 stained for immunohistochemistry. Rabbit anti-bovine OmpA antibody was used to identify
179 bovine *M. haemolytica* strains and rabbit anti-ovine OmpA antibody was used to identify
180 ovine *M. haemolytica* strains, at a dilution of 1:800. Heat-induced epitope retrieval was
181 performed using a Menarini Access Retrieval Unit and staining conducted using a Dako
182 Autostainer. Endogenous peroxidase was blocked with 0.3% (v/v) H₂O₂ in PBS. Following
183 incubation with the primary antibody, binding was identified by application of an anti-rabbit
184 HRP-labelled polymer and visualization with a REAL EnVision Peroxidase/DAB+ Detection
185 System (Dako; #K3468). Samples were subsequently counterstained with Gill's

186 haematoxylin, dehydrated, cleared and mounted in synthetic resin before sectioning. Tissue
187 sections were viewed with a Leica DM2000 microscope.

188 **Immunofluorescence microscopy**

189 At the stated time points post-infection, cultures were fixed by incubation with 4% (w/v)
190 paraformaldehyde for 15 min at room temperature and rinsed in PBS. Samples were
191 immunofluorescently stained as previously described in Cozens *et al.* Briefly, samples were
192 permeabilised using permabilization buffer (PBS with 0.5% [v/v] Triton X-100, 100 ml/ml
193 sucrose, 4.8 mg/ml HEPES, 2.9 mg/ml NaCl and 600 µg/ml MgCl₂, pH 7.2) for 10 min at
194 room temperature. Samples were blocked by incubation with PBS containing 0.05% (v/v)
195 Tween-20, 10% (v/v) goat serum and 1% (w/v) bovine serum albumin. The primary-
196 secondary antibody pairings were applied as follows. Bovine *M. haemolytica* strains were
197 detected using *M. haemolytica* antisera produced in cattle (1:50 dilution) and visualised with
198 goat anti-bovine-FITC antibody (1:400, Thermo Fisher #A18752). Ovine *M. haemolytica*
199 strains were detected using rabbit anti-ovine OmpA antibody (1:50 dilution) and visualised
200 with goat anti-rabbit-Alexa Fluor 488 (1:400 dilution; Thermo Fisher; #A-11008). Ciliated
201 cells were detected with mouse anti-β-tubulin antibody (1:50 dilution; Abcam; #ab131205).
202 Tight-junction formation was detected with mouse anti-ZO-1 antibody (1:50 dilution;
203 Thermo Fisher; #33910). Both anti-β-tubulin and anti-ZO-1 antibody binding was detected
204 with anti-mouse-Alexa Fluor 568 (1:400 dilution; Thermo Fisher; #A-11031). The cultures
205 were incubated with antibodies diluted in blocking buffer for 1 h at room temperature.
206 Samples were washed three times in PBS containing 0.05% (v/v) Tween-20 for 2 min
207 following each incubation. Blocking was repeated after each primary-secondary pairing.
208 Nuclei were stained with 300 nM 4',6 diamidino-2-phenylindole (DAPI) for 10 min.
209 Following staining, membranes were cut from their insert and mounted in Vectashield
210 mounting medium (Vector Laboratories). Samples were observed on a Leica DMI8

211 microscope. Z-stack orthogonal representation was observed on a Zeiss AxioObserver
212 ZIspinning disk confocal microscope. Analysis of captured images was performed using
213 ImageJ software.

214 **Scanning electron microscopy**

215 At the stated time points following infection, cultures were fixed in 1.5% (v/v)
216 glutaraldehyde in 0.1 M sodium cacodylate buffer for 1 h at 4°C. Samples were subsequently
217 rinsed three times with 0.1 M sodium cacodylate buffer and post-fixed in 1% (w/v) osmium
218 tetroxide for 1 h at room temperature. The cultures were washed three times for 10 min with
219 distilled water, stained with 0.5% (w/v) uranyl acetate for 1 h in the dark, washed twice with
220 distilled water and dehydrated through a series of increasing ethanol concentrations. The
221 samples were further dehydrated in hexamethyldisilazane before being placed in a desiccator
222 overnight. Membranes were cut from the inserts, mounted onto aluminium SEM stubs and
223 gold sputter-coated. The cultures were analysed on a Jeol 6400 scanning electron microscope
224 at 10 kV.

225 **Results**

226 ***M. haemolytica* infection of undifferentiated bovine bronchial epithelial cells**

227 The ability of *M. haemolytica* to adhere and colonise BBECs was first determined using
228 undifferentiated cultures. These cultures consisted of primary isolated BBEC cultures grown
229 in tissue culture inserts under submerged conditions. We have previously shown that under
230 these conditions BBEC form undifferentiated monolayers. Staining for β -tubulin was
231 indicative of cytoskeletal microtubules as opposed to cilia staining (Fig S1). However the
232 cultures did possess tight junctions, as identified using marker Zona Occludens-1 (ZO-1) (Fig
233 S2).

234 The undifferentiated BBEC cultures were apically infected with either *M. haemolytica* strain
235 PH2, an A1 serotype isolated from the lung of a pneumonic animal, or PH202, an A2
236 serotype isolated from the nasopharynx of a healthy animal. Adhesion and colonisation of
237 the bacteria was quantified following infection (Fig 1A). Initial adherence at 0.5-2 hours
238 post-infection (hpi) was comparable between the virulent PH2 strain and the commensal
239 PH202 strain. Approximately 1% of the inoculum initially adhered to the BBECs (Fig 1A
240 [i]). The majority of the inoculum was present in the apical washes (Fig 1A [ii]). At 24 hpi,
241 there is a significant increase in the number of PH2 present in the culture, particularly the
242 number of adherent bacteria (Two-way ANOVA), indicating that the strain was capable of
243 highly colonising undifferentiated BBECs. This colonisation was not replicated by PH202;
244 there was not a significant increase in either the number of adherent bacteria or bacteria
245 removed from the monolayer in the apical wash.

246 The localisation of bacteria adherent to undifferentiated BBECs was detected by labelling
247 with antisera raised against *M. haemolytica*. Epithelial cells were identified using β -tubulin
248 and DAPI (Fig 1B and Fig S1). Between 0.5-2 hpi, adherence was low for both strains. A
249 small population of bacteria was distributed on the apical surface of cells; however several
250 cultures were visually devoid of adherent bacteria. Conversely, after 24 hpi, PH2 was near-
251 confluent at numerous foci of infection present across the culture. These foci were separated
252 by areas of much lower colonisation density. This pattern was not replicated by PH202,
253 which at 24 hpi continued to show little to no evidence of adherence. Infected BBEC
254 cultures were also labelled for tight junctional protein ZO-1 to identify the effect of *M.*
255 *haemolytica* on tight junction integrity (Fig 1C). Tight junctions were shown to be stable
256 across all time points following infection with PH2 and PH202. However, at the foci of
257 infection, where PH2 was present at high number, tight junctions could not be observed. This
258 was determined to be due to damage to the colonised epithelial cells resulting in a disruption

259 in the integrity of the monolayer as opposed to direct targeting of the tight junction by PH2.

260 This will be discussed in greater detail below.

261 ***M. haemolytica* infection of differentiated bovine bronchial epithelial cells**

262 Adherence and colonisation of *M. haemolytica* was further determined using differentiated
263 BBEC cultures. Primary BBEC were grown at an ALI in order to stimulate polarisation of
264 airway epithelial cells into a culture which closely replicates the *in vivo* epithelium of the
265 bovine respiratory tract (Fig 2). At 21 days post-ALI, the BBEC cultures were shown to form
266 a pseudostratified columnar epithelium highly reminiscent to *ex vivo* tissue section (Fig 2A
267 [i] & 2B [i]). The apical surface of the BBEC cultures displayed both a high degree of
268 ciliation (Fig 2B [ii] & 2C [i]), and the formation of tight junction (Fig 2C [ii]), characteristic
269 of the bovine airway lumen. This model has previously been well characterised and was
270 shown to replicate other hallmarks of the airway epithelium, including the differentiation of
271 mucus-producing goblet cells and active mucociliary clearance.

272 The differentiated BBEC cultures were infected apically with either PH2 or PH202. The
273 number of bacteria present in the culture was quantified using the Miles and Misra method at
274 time points over a five day period (Fig 3). For both PH2 and PH202, initial adherence (0.5-2
275 hpi) was approximately 1% of the inoculum (Fig 3A); with the majority of the bacteria
276 removed following apical washing of the BBEC culture (Fig 3B). The number of adherent
277 PH2 increased within the BBEC cultures in a time-dependent manner from 6 hpi onwards
278 (Fig 3A). At 24 hpi, the number of PH2 adherent to the model was approximately 1800% the
279 initial inoculum. There was a subsequent decrease in the number of adherent PH2 at 48 hpi.
280 It is hypothesised that this decrease was due to removal of damaged BBECs following apical
281 washing, as discussed below. This increase in the number of adherent PH2 over time was
282 accompanied by an increase in the number of bacteria removed in the apical wash (Fig 3B).
283 Conversely, PH202 was not capable of colonising the BBEC model. In cultures derived from

284 two of the three donor animals, no viable bacteria could be detected at 120 hpi. In BBEC
285 cultures derived from a third animal, PH202 adhered to the culture at approximately 15% the
286 initial inoculum, 100-fold lower than the virulent PH2 strain (Fig 3A). This trend is
287 replicated in the number of bacteria removed by the apical wash (Fig 3B).

288 ***M. haemolytica* form foci of infection in differentiated bovine bronchial epithelial cells**

289 The distribution of *M. haemolytica* following infection of differentiated BBEC was
290 determined using several microscopic techniques (Fig 4 & 5). The adhesion of bacteria to the
291 apical surface was detected by labelling with antisera raised against *M. haemolytica*. From
292 0.5-6 hpi, PH2 was shown to be distributed across the apical surface of the culture at a low
293 density (Fig 4A & S3). The bacteria did not display a preference for ciliated or non-ciliated
294 cells during initial adherence. This observation was confirmed using SEM (Fig 4B & S4).
295 At 12 hpi, PH2 became increasing abundant at the apical surface, forming focal areas of
296 infection (Fig 4A [ii]). By this time point, PH2 had penetrated below the apical surface of the
297 BBEC cultures, as shown in histological sections labelled for *M. haemolytica* using an anti-
298 OmpA antibody (Fig 4C & S5). The density of PH2 at the foci of infection increased at 16
299 hpi (Fig 4A [iii]). These foci could be observed using SEM, in which PH2 was present in
300 near-confluent consolidations below the apical surface (Fig 4B [iii]). Bacteria could not be
301 observed at the apical surface in the proximity of the foci. Within the histological sections,
302 PH2 at the foci were shown to have penetrated the entirety of the epithelium to the basal
303 surface (Fig 4C [iii]). As exposure time increased, the number, size and density of the foci
304 increased. This phenomenon coincides with an increased quantity of bacteria recovered from
305 the apical surface (Fig 3A). By 24 hpi, foci were present at high numbers across the culture,
306 with large regions heavily colonised by PH2 below the apical surface (Fig 4C [v]). The
307 BBECs neighbouring the foci of infection did not display evidence of damage or cell death in
308 the initial 24 hours following challenge by PH2.

309 This pattern of infection observed following challenge of differentiated BBEC cultures by
310 virulent strain PH2 was not mimicked by commensal strain PH202 (Fig 5). The adherence of
311 PH202 could often be barely detected on the apical surface using immunofluorescence
312 labelling (Fig 5A) or SEM (Fig 5B). When PH202 was detected within the culture, the
313 bacteria were present on the apical surface at a low population density. Histological sections
314 of infected tissue confirmed that PH202 was not capable of penetrating the apical surface of
315 the culture (Fig 5C).

316 The effect of apical infecting with PH2 or PH202 on the integrity of the BBEC cultures was
317 investigated in histological sections (Fig 6 and S6). A semi-quantitative assessment of the
318 degree of infection was conducted at each time point from cultures derived from three
319 individual animals (Table 2). Evidence of infection following challenge by PH2 could be
320 observed by 12 hpi, at which individual foci of infection could be observed in regions across
321 the culture. The foci were increasingly abundant by 24 hpi. The BBECs at these foci
322 displayed cytopathic effects. Airway epithelial cells colonised by high numbers of PH2
323 became increasingly rounded and detached from the epithelium (Fig 6 [v]). Infected cells
324 displayed cytoskeletal staining for β -tubulin as opposed to cilia, indicating the cells are
325 becoming dedifferentiated. By 48 hpi, the integrity of the epithelium was drastically reduced,
326 and the majority of the culture was dislodged following apical washing (Fig S6). This may
327 account for the reduction in CFU at 48 hpi (Fig 3A). Epithelial cells still attached to the
328 epithelium appeared rounded (Fig S3) and were heavily colonised by bacteria (Fig S4). This
329 observation was not replicated following infection with PH202. Cultures remained healthy
330 until the time course was halted at 120 hpi (Fig S6). There was no evidence of cell rounding
331 or increased cell death, with the exception of animal 1, which at 120 hpi showed reduced
332 integrity of the cell layer. This was not observed in animal 2 or 3 (Table 2).

333 ***M. haemolytica* cause intracellular infections in differentiated bovine bronchial**
334 **epithelial cells**

335 Following labelling for PH2 within infected differentiated BBEC cultures, the distribution of
336 adherent bacteria appeared intracellular (Fig 4A [iv] & [v]). This was also observed in
337 histological sections (Fig 4C [v]). A gentamicin protection assay was used to confirm this
338 observation (Fig 7A). Following apical infection by PH2, a small subpopulation of
339 gentamicin-resistant (internalised) bacteria was enumerated at 12 hpi. This population
340 significantly increased by 24 hpi ($p < 0.001$, Two-way ANOVA). However, by 48 hpi this
341 number subsequently decreased, which coincided with the reduced integrity of the
342 epithelium. At this time point, high numbers of extracellular bacteria could be detected
343 across the remaining tissue (Fig S4). Gentamicin-resistant (internalised) PH202 could not be
344 detected at any time points following challenge.

345 Confocal microscopy confirmed the presence of intracellular *M. haemolytica* within BBECs
346 (Fig 7B). Z-stack projections of culture 24 hpi following challenge by PH2 confirmed the
347 presence of PH2 at near-confluent density confined within cell boundaries of both ciliated
348 and non-ciliated epithelial cells (Fig 7B). This phenomenon was confirmed using SEM (Fig
349 7C). Epithelial plasma membrane projections could be observed in proximity to PH2 at the
350 surface of a non-ciliated epithelial cell, suggesting the bacteria was being internalised via
351 macropinocytosis (Fig 7C [i]). Internalised bacteria could also be observed at high number
352 within epithelial cells when the apical membrane was removed (Fig 7C [ii]). This suggested
353 *M. haemolytica* penetrated the apical surface via transcytosis, and was capable of intracellular
354 survival within airway epithelial cells.

355 ***M. haemolytica* does not affect tight junction integrity in differentiated bovine bronchial**
356 **epithelial cells**

357 The integrity of tight junctions between BBECs within infected cultures was assessed
358 following challenge by PH2 and PH202 (Fig 8). At early time points (0.5-20 hpi), tight
359 junctions could be observed in the BBEC cultures, there was no detectable effect on the
360 integrity of the junctional complexes due to colonisation of *M. haemolytica*. This observation
361 was true for both the foci of infections and cells which were not colonised. Tight junctions
362 however did appear effected at later time points following challenge by PH2 (24 hpi).
363 Rounded epithelial cells at the foci of infection displayed reduced integrity of tight junctions
364 at cell-to-cell borders (Fig 8A [v]). From 48-120 hpi, the epithelium was severely
365 deteriorated and tight junctions could not be observed (Fig S7). PH202 infection however
366 had no effect on the presence of tight junctions. These observations were confirmed by the
367 measuring the TEER of the culture following infection (Fig 8B). Challenge by PH202 had no
368 detectable effect on the TEER of the culture. Conversely, PH2 caused a significant reduction
369 in TEER at 48 hpi ($p < 0.001$, Two-way ANOVA). This indicated that colonisation by PH2
370 disturbed the integrity of the tight junctions.

371 This damage to junctional complexes was determined to be due to damage to the epithelium
372 as opposed to direct targeting of tight junctions by *M. haemolytica*. Lipoxin A4 was used to
373 stimulate tight junction formation [46]. Following treatment with lipoxin A4, TEER was
374 increased within the BBEC culture, and labelling for ZO-1 became increasingly prominent, in
375 a dose-dependent manner (data not shown). It was hypothesised that if PH2 was targeting
376 tight junctions to penetrate the apical surface to colonise the culture, colonisation would be
377 reduced following treatment. However, lipoxin A4 pre-treatment of BBECs did not affect the
378 number of CFU adherent to the culture following challenge by PH2 24 hpi (Fig 8C).

379 **Serotype and host species of origin affects the capacity of *M. haemolytica* to colonise**
380 **differentiated bovine bronchial epithelial cells**

381 Differentiated BBECs were infected with eight strains of *M. haemolytica*, listed in Table 1.
382 These strains were isolated from healthy and pneumonic cattle and sheep. Cultures were
383 infected apically with 2.5×10^7 cfu/insert, and colonisation was quantified at 2, 24 and 72 hpi
384 (Fig 9A [i] & S8). The number of CFU present in the apical wash was also enumerated (Fig
385 9 [ii] 7 S8). At 2 hpi, there was no significant difference in the adherence efficiency between
386 all eight strains (Two-way ANOVA). There was little evidence of bacteria present on the
387 apical surface as observed using SEM at 2 hpi (Fig S10 & S11). By 24 hpi however, both the
388 virulent A1 strains isolated from pneumonic cattle (PH2 and PH376) and virulent A2 strains
389 isolated from pneumonic sheep (PH278 and PH372) were capable of successfully colonising
390 the BBEC cultures. This colonisation was observed as foci of infection below the apical
391 surface, as described for PH2 (Fig 10A). The apical surfaces surrounding the foci were
392 largely devoid of adherent bacteria (Fig 10B). Adherence of virulent bovine strains to the
393 BBEC was approximately 10-fold higher in comparison to virulent ovine strains. This was
394 reflected in a higher number of foci of infection present after challenge with PH2 and PH376.
395 At 72 hpi, significant deterioration was observed in epithelia infected by all virulent strains,
396 as displayed within histological sections and SEM (Fig 10). This was reflected in a reduction
397 in the TEER (Fig 9B). A semi-quantitative scoring of this damage using histological sections
398 was performed (Table 3). Deterioration following infection by virulent ovine strains,
399 particularly PH372 was less prominent in comparison to the bovine strains, which appeared
400 more invasive to BBEC cultures.

401 Neither the commensal bovine (PH202 and PH210, A2 serotype) or ovine strains (PH62 and
402 PH346, A12 serotype) displayed a significant increases in adherence efficiency between 2 to
403 24 hpi (Two-way ANOVA; Fig 9). There was a slight increase in CFU present in the culture

404 for all commensal strains by 72 hpi; however the number of bacteria within the culture was
405 significantly lower in comparison to all strains isolated from pneumonic animals. Visually,
406 BBEC cultures infected by commensal strains did not present overt evidence of colonisation
407 or damage to the epithelium (Fig 10), and the TEER was not affected (Fig 9B). Foci of
408 infection could be observed in individual cultures for PH210, PH62 and PH346 (Table 3).
409 However these were in isolated incidence and were present at a much lower number in
410 comparison to virulent strains. Such foci were located towards the border regions of the foci,
411 at which the epithelium can present evidence of damage. This data suggests that virulent
412 strains were capable of successfully colonising differentiated BBEC following apical
413 infection. Conversely, commensal strains isolated from the nasopharynx of healthy animals
414 were not capable of successfully colonising the model to a high degree.

415 **Discussion**

416 The aim of the study was to investigate the interaction between pathogenic and virulent
417 strains of *M. haemolytica* with the bovine airway epithelium using a differentiated cell model,
418 in order to have a better understanding of the events of BRD. Differentiated airway epithelial
419 models have been utilised previously to study a number of bacterial pathogens, including
420 *Pseudomonas aeruginosa* [47-49], *Haemophilus influenzae* [50-52], *Neisseria meningitidis*
421 [53] and *Mycoplasma pneumoniae* [38, 41]. To our knowledge, this investigation is the first
422 to utilise a differentiated cell model to study the interaction of *M. haemolytica* with the
423 bovine airway epithelium. This has allowed the adherence, colonisation and traversal of the
424 epithelium by *M. haemolytica* to be studied in a model which displayed the characteristic
425 defence mechanisms associated with the respiratory tract. The model provides an alternative
426 to animal models, which are costly and time-intensive, and are contrary to the three R's
427 principles.

428 Submerged BBECs have routinely been utilised to study the adherence of *M. haemolytica*
429 [30, 54-56]. However, submerged epithelial cultures are undifferentiated [57], and as such do
430 not replicate the complexity of the airway epithelium [58]. Bovine bronchial epithelial cells
431 can be stimulated to differentiate into a more representative model of the *in vivo*
432 microenvironment through exposure to the atmosphere [36, 37, 59]. The methodology for
433 differentiation of bovine airway epithelial cells have been fully optimised [44] and the model
434 well-characterised [45]. The differentiated BBEC model has been shown to replicate the
435 hallmark defences of the respiratory tract, including active mucociliary clearance. These
436 mechanisms actively prevent colonisation of invading pathogens, and are important
437 considerations when modelling bacterial interactions within the airway. Tight junctions
438 present in the differentiated BBEC also allowed for the identification of invasion of the
439 pathogen through the apical barrier (Fig 4C) into the sub-apical epithelium. Our model
440 therefore allows for these defence mechanisms to be considered when assessing colonisation
441 of *M. haemolytica*, and as such provides an excellent model to characterise *M. haemolytica*-
442 host interaction in the bovine airway epithelium.

443 A direct comparison of the ability of *M. haemolytica* to colonise differentiated and
444 undifferentiated BBEC cultures was made in this investigation (Fig 1 & Fig 3). Initial
445 adherence of *M. haemolytica* to BBEC was comparable between the two models. As
446 undifferentiated BBEC cultures do not possess cilia, it was inferred that adhesion is not
447 specific to either ciliated or unciliated cells. This was confirmed using immunofluorescence
448 and SEM (Fig 4). In both models PH2, isolated from lung of pneumonic cattle, was capable
449 of heavily colonising cells by 24 hpi. Adherence at 24 hpi was 10-fold higher in the
450 differentiated model in comparison to the undifferentiated model. This may be due to the
451 increased thickness of the epithelium in the differentiated model, where a columnar,
452 pseudostratified morphology was formed, stereotypical for the airway epithelium (Fig 2), as

453 opposed to a two-dimensional monolayer. This provided a larger 3-D architecture for the
454 bacteria to adhere, highlighting the importance of cell differentiation when investigating
455 epithelial colonisation.

456 The differentiated BBEC was initially infected with two strains of *M. haemolytica*, PH2, a
457 bovine isolate from the lung of a pneumonic animal, and PH202, a bovine isolate from the
458 nasopharynx of a healthy animal (Fig 3). PH2 is an A1 serotype strain, which is the major
459 cause of pneumonic pasteurellosis in cattle [60, 61]. PH202 is an A2 serotype, a
460 predominately non-pathogenic serotype present as a commensal species in cattle [29, 61]. A1
461 and A2 are the most prevalent serotypes worldwide [29, 60]. Both strains have previously
462 been shown to adhere to undifferentiated ovine bronchial epithelial cells [62]. Initial
463 adherence of both PH2 and PH202 to differentiated BBEC cultures was low (Fig 3). At early
464 time points (0.5-6 hpi), bacteria associated with the culture were distributed at a low density
465 across the apical surface (Figs 4A & 5A). However, following further incubation PH2
466 became increasingly abundant. Penetration of PH2 below the apical surface of the culture
467 was identified by 12 hpi; suggesting *M. haemolytica* A1 is capable of traversing epithelial
468 tight junctions (Fig 4C). This coincided with a significant increase in the number of adherent
469 bacteria (Fig 3). At the foci of infection, PH2 replicated to a high density below the apical
470 surface (Fig 4). Such foci have previously been described for *H. influenza* [51] and *M.*
471 *pneumoniae* [41]. The number of foci increased with exposure time, as did the number of
472 PH2 present in the systems which were not closely associated with tissue (Fig 3). This
473 provided evidence that the bacteria disseminated from the foci to re-infecting other regions of
474 the culture. From 48 hpi onwards, the majority of the epithelium was heavily infected, and
475 distinct foci no longer observed.

476 Conversely, A2 commensal strain PH202 was not capable of colonising the differentiated
477 BBEC model. Although initial adherence of the bacterium could be detected at early time

478 points post-infection (Fig 3), there was no evidence of PH202 penetrating the apical surface
479 (Fig 5C). In tissue derived from two of the three animals, viable PH202 could not be
480 recovered from the culture at the end point of the infection. This finding indicated that the
481 differentiated model actively prevented colonisation by the bacteria. This may be due to
482 mucociliary clearance which actively removes invading pathogens [63, 64]. Alternatively,
483 BBECs are known to produce anti-bacterial peptides, such as tracheal antimicrobial peptide
484 (TAP), in response to bacterial products including LPS [65-67]. This peptide has shown to
485 be bactericidal against *M. haemolytica* [68]. The variation observed in the ability of the A1
486 and A2 bacteria to adhere to the culture may provide insight into the selective explosion of
487 the A1 population over A2 strains, resulting in infection in the lower respiratory tract during
488 pneumonic pasteurellosis [27].

489 Following extended co-culture of differentiated BBECs and PH2 (48-120 hpi), there was
490 significant evidence of damage present in airway epithelial cells. By 24 hpi, there was cell
491 rounding and detachment in BBECs heavily colonised by *M. haemolytica* (Fig 6). This
492 phenomenon was more pronounced at 48 hpi, where a large number of cells were readily
493 detached from culture following apical washing (Fig S6). This response was only observed
494 following PH202 infection in tissue derived from one of three animals at 120 hpi (Table 2).
495 Similar cytopathic effects in epithelial cells have been observed in response to other bacterial
496 pathogens, including *P. aeruginosa* [69] and *Klebsiella pneumoniae* [70]. This may mimic
497 events *in vivo*. Clinical signs of *M. haemolytica* include pulmonary lesions, and necrosis and
498 desquamation can also be observed at the bronchial epithelium [29]. The cause of the
499 induced cell death in the model is unknown. Major *Mannheimia* virulence factors
500 lipopolysaccharide (LPS) and leukotoxin have been shown to not cause necrosis or apoptosis
501 in bovine pulmonary epithelial cells [71]. Epithelial cell death observed in the system may

502 however be due to the innate immune response following bacterial infection, resulting in the
503 sloughing off of infected cells [72].

504 In this study we presented evidence that *M. haemolytica* A1 strain PH2 may be internalised
505 by airway epithelial cells following infection (Fig 7). Internalisation of *M. haemolytica* A1
506 by BBECs has not been previously reported. A small subpopulation of PH2 was identified to
507 be resistant following treatment with gentamicin, indicative of the presence of intracellular
508 bacteria (Fig 7A). This was confirmed using a number of microscopy techniques (Figs 7B
509 and 7C). Within BBECs, intracellular PH2 could be detected from 12 hpi. This number
510 appeared to peak at 24 hpi (Fig 7A). Electron microscopy suggests that internalisation of
511 PH2 in epithelial cells may be occurring through macropinocytosis (Fig 7C). This has
512 previously been observed for *H. influenzae* [51]. *M. haemolytica* was present at high density
513 within cell boundaries (Fig 7B), suggesting that once internalised PH2 is capable of survival
514 and replication within host cells. *M. haemolytica* A1 may invade BBECs in order to gain
515 access to sub-epithelial spaces thorough transcytosis of the epithelium. An intracellular
516 phase during infection may also allow for persistence or evasion of aspects of host immunity,
517 such as humoral and complement-attack or mucociliary clearance [73].

518 Tight junctions create a physiochemical barrier to prevent the invasion of pathogens from the
519 lumen of the airway to the interstitial compartment [74, 75]. However, several bacteria are
520 capable of disrupting the junctional complexes during paracytosis [76, 77]. This was not
521 observed following colonisation of either PH2 or PH202 (Fig 8). Tight junctions were
522 present following challenge by *M. haemolytica*, with no detectable reduction in integrity by
523 24 hpi (Fig 8A). This was confirmed by measuring the TEER of the culture (Fig 8B). There
524 was however a detectable decrease in the number of tight junctions present by 48 hpi with
525 PH2. However this was due to significant damage to the epithelium following infection,
526 particularly at the apical surface (Fig S6). The addition of lipoxin A4, which stimulates

527 expression of ZO-1, has previously been shown to prevent the invasion and transmigration of
528 *P. aeruginosa* [78]. However stimulation of BBEC cultures did not prevent colonisation by
529 PH2, despite enhancing the integrity of tight junctions (Fig 8C), further suggesting that tight
530 junctions are not targeted by *M. haemolytica*. It is hypothesised therefore that transmigration
531 of the bacterium through the apical surface of the epithelium occurred via transcytosis, but
532 not through paracellular transport.

533 The pattern of infection of PH2 was replicated using a second bovine A1 isolate PH376.
534 Both strains colonised the BBEC cultures to a comparable degree (Fig 9A), forming
535 morphologically similar infection foci (Fig 10) beneath the apical surface at 24 hpi.
536 Significant damage to the tissue was detected at 72 hpi with both strains (Fig S12). A2
537 bovine isolate PH210, in agreement with PH202, was not capable of forming foci of infection
538 stereotypical of A1 strains (Fig 10). The model was further challenged with four ovine
539 isolates (Fig 9 & 10). Two strains (PH278 and PH372) were representative of A2 ovine
540 strains, the major causative agent of pneumonia in sheep [29, 60]. As with the bovine
541 isolates, the virulent strains were capable of colonising the model to form foci of infection.
542 The A2 bovine isolates behaved differently from ovine A2 isolates when co-cultured with the
543 model (Fig 9). This is to be expected as the outer-membrane protein profiles differ between
544 the two groups [21]. Cultures were also infected with two A12 strains (PH62 and PH346),
545 which are traditionally not associated with disease. The commensal A12 strains failed to
546 colonise the cultures to a similar degree (Fig 9). Adherence to bovine airway epithelial cells
547 by virulent ovine isolates was approximately 10-fold lower in comparison to virulent bovine
548 isolates (Fig 9). This suggests that host specificity in *M. haemolytica* strains was partly
549 dependent on specific cell-surface structures present on differentiated BBECs. This
550 difference in pathogenesis between serotypes is likely due to variation in the LPS profile [21,
551 22], outer-membrane proteins [21] and allelic variation in a number of virulence genes such

552 as *lktA* [23], *ompA* [24]. In conclusion, variation in disease pathogenesis *in vivo* due to
553 serotype and host specificity is reflected in the degree of colonisation within the
554 differentiated BBEC culture.

555 In this study we have characterised the host-pathogen interactions between BBECs grown at
556 an ALI with various serotypes of *M. haemolytica*. The model used to investigate the
557 infection *in vitro* has been shown to be highly representative of the *in vivo* epithelium,
558 providing insight into the pathogenesis of *M. haemolytica* during pneumonic pasteurellosis in
559 the context of host defence mechanisms, such as tight junctions and mucociliary clearance.
560 *M. haemolytica* A1 was capable of highly colonising the model, causing extensive damage to
561 the host epithelium. This occurred at foci of infection, below the apical surface of the tissue.
562 Tight junctions in the epithelium were bypassed using transcytosis, but not paracytosis. *M.*
563 *haemolytica* A2 was not capable of replicating this colonisation. This may account for the
564 occurrence of lower respiratory tract infection following the shift from A2 to A1 population
565 in cattle prior to onset of pneumonic pasteurellosis. The BBEC model was further challenged
566 using a panel of isolates, and the degree of pathogenesis was dependent on both serotype and
567 host species. This investigation provides the first insight into the route of infection of *M.*
568 *haemolytica* in a differentiated model of the bovine airway epithelium.

569 **Acknowledgements**

570 We thank Ms Margaret Mullin and Ms Lynne Stevenson (both University of Glasgow) for
571 assistance with electron microscopy and histology, respectively.

572 **References**

- 573 1. Jeyaseelan S, Sreevatsan S, Maheswaran SK. Role of *Mannheimia haemolytica*
574 leukotoxin in the pathogenesis of bovine pneumonic pasteurellosis. *Anim Health Res Rev.*
575 2002; 3: 69-82. pmid: 12665107.
- 576 2. Jones C, Chowdhury S. A review of the biology of bovine herpesvirus type 1 (BHV-
577 1), its role as a cofactor in the bovine respiratory disease complex and development of
578 improved vaccines. *Anim Health Res Rev.* 2007; 8: 187-205. doi:
579 10.1017/S146625230700134X. pmid: 18218160.
- 580 3. Singh K, Ritchey JW, Confer AW. *Mannheimia haemolytica*: bacterial-host
581 interactions in bovine pneumonia. *Vet Pathol.* 2011; 48: 338-48. doi:
582 10.1177/0300985810377182. pmid: 20685916.
- 583 4. Czuprynski CJ. Host response to bovine respiratory pathogens. *Anim Health Res Rev.*
584 2009; 10: 141-3. doi: 10.1017/S1466252309990181. pmid: 20003650.
- 585 5. Panciera RJ, Confer AW. Pathogenesis and pathology of bovine pneumonia. *Vet Clin*
586 *North Am Food Anim Pract.* 2010; 26: 191-214. pmid: 20619179.
- 587 6. Srikumaran S, Kelling CL, Ambagala A. Immune evasion by pathogens of bovine
588 respiratory disease complex. *Anim Health Res Rev.* 2007; 8: 215-29. doi:
589 10.1017/S1466252307001326. pmid: 18218162.
- 590 7. Gershwin LJ, Berghaus LJ, Arnold K, Anderson ML, Corbeil LB. Immune
591 mechanisms of pathogenetic synergy in concurrent bovine pulmonary infection with
592 *Haemophilus somnus* and bovine respiratory syncytial virus. *Vet Immunol Immunopathol.*
593 2005; 107: 119-30. doi: 10.1016/j.vetimm.2005.04.004. pmid: 15979157.
- 594 8. Gershwin LJ, Van Eenennaam AL, Anderson ML, McEligot HA, Shao MX, Toaff-
595 Rosenstein R, et al. Single pathogen challenge with agents of the bovine respiratory disease

- 596 complex. PLoS One. 2015; 10: e0142479. doi: 10.1371/journal.pone.0142479. pmid:
597 26571015.
- 598 9. Hodgson PD, Aich P, Manuja A, Hokamp K, Roche FM, Brinkman FS, et al. Effect
599 of stress on viral-bacterial synergy in bovine respiratory disease: novel mechanisms to
600 regulate inflammation. Comp Funct Genomics. 2005; 6: 244-50. doi: 10.1002/cfg.474. pmid:
601 18629190.
- 602 10. Rice JA, Carrasco-Medina L, Hodgins DC, Shewen PE. *Mannheimia haemolytica* and
603 bovine respiratory disease. Anim Health Res Rev. 2007; 8: 117-28. doi:
604 10.1017/s1466252307001375.
- 605 11. Whiteley LO, Maheswaran SK, Weiss DJ, Ames TR, Kannan MS. *Pasteurella*
606 *haemolytica* A1 and bovine respiratory disease: pathogenesis. J Vet Intern Med. 1992; 6: 11-
607 22. pmid: 1548621.
- 608 12. Confer AW. Update on bacterial pathogenesis in BRD. Anim Health Res Rev. 2009;
609 10: 145-8. doi: 10.1017/S1466252309990193. pmid: 20003651.
- 610 13. Frank GH. Pasteurellosis of cattle. In: Adlam C, Rutter JM, editors. *Pasteurella* and
611 Pasteurellosis. London: Academic Press; 1989. p. 197-222.
- 612 14. Angen O, Muters R, Caugant DA, Olsen JE, Bisgaard M. Taxonomic relationships of
613 the [*Pasteurella*] *haemolytica* complex as evaluated by DNA-DNA hybridizations and 16S
614 rRNA sequencing with proposal of *Mannheimia haemolytica* gen. nov., comb. nov.,
615 *Mannheimia granulomatis* comb. nov., *Mannheimia glucosida* sp. nov., *Mannheimia*
616 *ruminalis* sp. nov. and *Mannheimia varigena* sp. nov. Int J Syst Bacteriol. 1999; 49 Pt 1: 67-
617 86. doi: 10.1099/00207713-49-1-67. pmid: 10028248.
- 618 15. Griffin D, Chengappa MM, Kuszak J, McVey DS. Bacterial pathogens of the bovine
619 respiratory disease complex. Vet Clin North Am Food Anim Pract. 2010; 26: 381-94. doi:
620 10.1016/j.cvfa.2010.04.004. pmid: 20619191.

- 621 16. Klima CL, Alexander TW, Read RR, Gow SP, Booker CW, Hannon S, et al. Genetic
622 characterization and antimicrobial susceptibility of *Mannheimia haemolytica* isolated from
623 the nasopharynx of feedlot cattle. *Vet Microbiol.* 2011; 149: 390-8. doi:
624 10.1016/j.vetmic.2010.11.018. pmid: 21146332.
- 625 17. Adlam C, Knights JM, Mugridge A. Production of colomic acid by *Pasteurella*
626 *haemolytica* serotype A2 organisms. *FEMS Microbiol Lett.* 1987; 42: 23-5.
- 627 18. Adlam C, Knights JM, Mugridge A, Lindon JC, Baker PR, Beesley JE, et al.
628 Purification, characterization and immunological properties of the serotype-specific capsular
629 polysaccharide of *Pasteurella haemolytica* (serotype A1) organisms. *J Gen Microbiol.* 1984;
630 130: 2415-26. doi: 10.1099/00221287-130-9-2415. pmid: 6502135.
- 631 19. Davies RL, Arkinsaw S, Selander RK. Evolutionary genetics of *Pasteurella*
632 *haemolytica* isolates recovered from cattle and sheep. *Infect Immun.* 1997; 65: 3585-93.
633 pmid: 9284123.
- 634 20. Klima CL, Cook SR, Zaheer R, Laing C, Gannon VP, Xu Y, et al. Comparative
635 genomic analysis of *Mannheimia haemolytica* from bovine sources. *PLoS One.* 2016; 11:
636 e0149520. doi: 10.1371/journal.pone.0149520. pmid: 26926339.
- 637 21. Davies RL, Donachie W. Intra-specific diversity and host specificity within
638 *Pasteurella haemolytica* based on variation of capsular polysaccharide, lipopolysaccharide
639 and outer-membrane proteins. *Microbiology.* 1996; 142: 1895-907. doi:
640 doi:10.1099/13500872-142-7-1895.
- 641 22. Lacroix RP, Duncan JR, Jenkins RP, Leitch RA, Perry JA, Richards JC. Structural
642 and serological specificities of *Pasteurella haemolytica* lipopolysaccharides. *Infect Immun.*
643 1993; 61: 170-81. pmid: 8418039.
- 644 23. Davies RL, Whittam TS, Selander RK. Sequence diversity and molecular evolution of
645 the leukotoxin (lktA) gene in bovine and ovine strains of *Mannheimia (Pasteurella)*

- 646 *haemolytica*. J Bacteriol. 2001; 183: 1394-404. doi: 10.1128/jb.183.4.1394-1404.2001. pmid:
647 11157953.
- 648 24. Davies RL, Lee I. Sequence diversity and molecular evolution of the heat-modifiable
649 outer membrane protein gene (*ompA*) of *Mannheimia (Pasteurella) haemolytica*,
650 *Mannheimia glucosida*, and *Pasteurella trehalosi*. J Bacteriol. 2004; 186: 5741-52. pmid:
651 15317779.
- 652 25. Lee I, Davies RL. Evidence for a common gene pool and frequent recombinational
653 exchange of the *tbpBA* operon in *Mannheimia haemolytica*, *Mannheimia glucosida* and
654 *Bibersteinia trehalosi*. Microbiology. 2011; 157: 123-35. pmid: 20884693.
- 655 26. Ayalew S, Blackwood ER, Confer AW. Sequence diversity of the immunogenic outer
656 membrane lipoprotein PlpE from *Mannheimia haemolytica* serotypes 1, 2, and 6. Vet
657 Microbiol. 2006; 114: 260-8. doi: 10.1016/j.vetmic.2005.11.067. pmid: 16386856.
- 658 27. Grey CL, Thomson RG. *Pasteurella haemolytica* in the tracheal air of calves. Can J
659 Comp Med. 1971; 35: 121-8. pmid: 4253460.
- 660 28. Lawrence PK, Nelson WR, Liu W, Knowles DP, Foreyt WJ, Srikumaran S. beta(2)
661 integrin Mac-1 is a receptor for *Mannheimia haemolytica* leukotoxin on bovine and ovine
662 leukocytes. Vet Immunol Immunopathol. 2008; 122: 285-94. doi:
663 10.1016/j.vetimm.2007.12.005. pmid: 18262657.
- 664 29. Zecchinon L, Fett T, Desmecht D. How *Mannheimia haemolytica* defeats host
665 defence through a kiss of death mechanism. Vet Res. 2005; 36: 133-56. doi:
666 10.1051/vetres:2004065. pmid: 15720968.
- 667 30. Kisiela DI, Czuprynski CJ. Identification of *Mannheimia haemolytica* adhesins
668 involved in binding to bovine bronchial epithelial cells. Infect Immun. 2009; 77: 446-55. doi:
669 10.1128/IAI.00312-08. pmid: PMC2612293.

- 670 31. Lin C, Agnes JT, Behrens N, Shao M, Tagawa Y, Gershwin LJ, et al. *Histophilus*
671 *somni* stimulates expression of antiviral proteins and inhibits BRSV replication in bovine
672 respiratory epithelial cells. PLoS One. 2016; 11: e0148551. doi:
673 10.1371/journal.pone.0148551. pmid: 26859677.
- 674 32. Rivera-Rivas JJ, Kisiela D, Czuprynski CJ. Bovine herpesvirus type 1 infection of
675 bovine bronchial epithelial cells increases neutrophil adhesion and activation. Vet Immunol
676 Immunopathol. 2009; 131: 167-76. doi: 10.1016/j.vetimm.2009.04.002. pmid: 19406483.
- 677 33. Abraham G, Zizzadoro C, Kacza J, Ellenberger C, Abs V, Franke J, et al. Growth and
678 differentiation of primary and passaged equine bronchial epithelial cells under conventional
679 and air-liquid-interface culture conditions. BMC Vet Res. 2011; 7: 26. doi: 10.1186/1746-
680 6148-7-26. pmid: PMC3117700.
- 681 34. Balder R, Krunkosky TM, Nguyen CQ, Feezel L, Lafontaine ER. Hag mediates
682 adherence of *Moraxella catarrhalis* to ciliated human airway cells. Infect Immun. 2009; 77:
683 4597-608. doi: 10.1128/IAI.00212-09. pmid: PMC2747927.
- 684 35. Bateman AC, Karasin AI, Olsen CW. Differentiated swine airway epithelial cell
685 cultures for the investigation of influenza A virus infection and replication. Influenza Other
686 Respir Viruses. 2013; 7: 139-50. doi: 10.1111/j.1750-2659.2012.00371.x. pmid:
687 PMC3443301.
- 688 36. Goris K, Uhlenbruck S, Schwegmann-Wessels C, Köhl W, Niedorf F, Stern M, et al.
689 Differential sensitivity of differentiated epithelial cells to respiratory viruses reveals different
690 viral strategies of host infection. J Virol. 2009; 83: 1962-8. doi: 10.1128/jvi.01271-08. pmid:
691 19052091.
- 692 37. Kirchhoff J, Uhlenbruck S, Goris K, Keil GM, Herrler G. Three viruses of the bovine
693 respiratory disease complex apply different strategies to initiate infection. Vet Res. 2014; 45:
694 20. doi: 10.1186/1297-9716-45-20. pmid: 24548739.

- 695 38. Krunkosky TM, Jordan JL, Chambers E, Krause DC. *Mycoplasma pneumoniae* host–
696 pathogen studies in an air–liquid culture of differentiated human airway epithelial cells.
697 Microb Pathog. 2007; 42: 98-103. doi: 10.1016/j.micpath.2006.11.003. pmid: 17261358.
- 698 39. Lam E, Ramke M, Groos S, Warnecke G, Heim A. A differentiated porcine bronchial
699 epithelial cell culture model for studying human adenovirus tropism and virulence. J Virol
700 Methods. 2011; 78: 117-23. doi: 10.1016/j.jviromet.2011.08.025. pmid: 21907242.
- 701 40. Palermo LM, Porotto M, Yokoyama CC, Palmer SG, Mungall BA, Greengard O, et
702 al. Human parainfluenza virus infection of the airway epithelium: viral hemagglutinin-
703 neuraminidase regulates fusion protein activation and modulates infectivity. J Virol. 2009;
704 83: 6900-8. doi: 10.1128/jvi.00475-09. pmid: 19386708.
- 705 41. Prince OA, Krunkosky TM, Krause DC. *In vitro* spatial and temporal analysis of
706 *Mycoplasma pneumoniae* colonization of human airway epithelium. Infect Immun. 2014; 82:
707 579-86. doi: 10.1128/IAI.01036-13. pmid: 24478073.
- 708 42. Schwab UE, Fulcher ML, Randell SH, Flaminio MJ, Russell DG. Equine bronchial
709 epithelial cells differentiate into ciliated and mucus producing cells *in vitro*. In Vitro Cell Dev
710 Biol Anim. 2010; 46: 102-6. doi: 10.1007/s11626-009-9258-6. pmid: 19915928.
- 711 43. Villenave R, Thavagnanam S, Sarlang S, Parker J, Douglas I, Skibinski G, et al. *In*
712 *vitro* modeling of respiratory syncytial virus infection of pediatric bronchial epithelium, the
713 primary target of infection in vivo. Proc Natl Acad Sci USA. 2012; 109. doi:
714 10.1073/pnas.1110203109. pmid: 22411804.
- 715 44. Cozens D, Grahame E, Sutherland E, Taylor G, Berry C, Davies R. Development and
716 optimization of a differentiated airway epithelial cell model of the bovine respiratory tract.
717 Sci Rep. 2017; (submitted).

- 718 45. Cozens D, Sutherland E, Marchesi F, Taylor G, Berry CC, Davies RL. Temporal
719 differentiation of bovine airway epithelial cells grown at an air-liquid interface. *J Histochem*
720 *Cytochem.* 2017; (submitted).
- 721 46. Grumbach Y, Quynh NV, Chiron R, Urbach V. LXA4 stimulates ZO-1 expression
722 and transepithelial electrical resistance in human airway epithelial (16HBE14o-) cells. *Am J*
723 *Physiol Lung Cell Mol Physiol.* 2009; 296: L101-8. doi: 10.1152/ajplung.00018.2008. pmid:
724 18849442.
- 725 47. Garcia-Medina R, Dunne WM, Singh PK, Brody SL. *Pseudomonas aeruginosa*
726 acquires biofilm-like properties within airway epithelial cells. *Infect Immun.* 2005; 73: 8298-
727 305. doi: 10.1128/IAI.73.12.8298-8305.2005. pmid: PMC1307054.
- 728 48. Bucior I, Pielage JF, Engel JN. *Pseudomonas aeruginosa* pili and flagella mediate
729 distinct binding and signaling events at the apical and basolateral surface of airway
730 epithelium. *PLoS Pathog.* 2012; 8: e1002616. doi: 10.1371/journal.ppat.1002616. pmid:
731 22496644.
- 732 49. Halldorsson S, Gudjonsson T, Gottfredsson M, Singh PK, Gudmundsson GH,
733 Baldursson O. Azithromycin maintains airway epithelial integrity during *Pseudomonas*
734 *aeruginosa* infection. *Am J Respir Cell Mol Biol.* 2010; 42: 62-8. doi: 10.1165/rcmb.2008-
735 0357OC. pmid: 19372247.
- 736 50. Ren D, Nelson KL, Uchakin PN, Smith AL, Gu X-X, Daines DA. Characterization of
737 extended co-culture of non-typeable *Haemophilus influenzae* with primary human respiratory
738 tissues. *Exp Biol Med.* 2012; 237: 540-7. doi: 10.1258/ebm.2012.011377.
- 739 51. Ketterer MR, Shao JQ, Hornick DB, Buscher B, Bandi VK, Apicella MA. Infection of
740 primary human bronchial epithelial cells by *Haemophilus influenzae*: macropinocytosis as a
741 mechanism of airway epithelial cell entry. *Infect Immun.* 1999; 67: 4161-70. pmid:
742 10417188.

- 743 52. van Schilfgaarde M, van Alphen L, Eijk P, Everts V, Dankert J. Paracytosis of
744 *Haemophilus influenzae* through cell layers of NCI-H292 lung epithelial cells. *Infect Immun.*
745 1995; 63: 4729-37. pmid: 7591129.
- 746 53. Sutherland TC, Quattroni P, Exley RM, Tang CM. Transcellular passage of *Neisseria*
747 *meningitidis* across a polarized respiratory epithelium. *Infect Immun.* 2010; 78: 3832-47. doi:
748 10.1128/iai.01377-09. pmid: 20584970.
- 749 54. Galdiero M, Pisciotta MG, Marinelli A, Petrillo G, Galdiero E. Coinfection with
750 BHV-1 modulates cell adhesion and invasion by *P. multocida* and *Mannheimia (Pasteurella)*
751 *haemolytica*. *New Microbiol.* 2002; 25: 427-36. pmid: 12437222.
- 752 55. N'Jai A U, Rivera J, Atapattu DN, Owusu-Ofori K, Czuprynski CJ. Gene expression
753 profiling of bovine bronchial epithelial cells exposed *in vitro* to bovine herpesvirus 1 and
754 *Mannheimia haemolytica*. *Vet Immunol Immunopathol.* 2013; 155: 182-9. doi:
755 10.1016/j.vetimm.2013.06.012. pmid: 23890750.
- 756 56. Boukahil I, Czuprynski CJ. *Mannheimia haemolytica* biofilm formation on bovine
757 respiratory epithelial cells. *Vet Microbiol.* 2016; 197: 129-36. doi:
758 10.1016/j.vetmic.2016.11.012. pmid: 27938674.
- 759 57. Ostrowski LE, Nettekheim P. Inhibition of ciliated cell differentiation by fluid
760 submersion. *Exp Lung Res.* 1995; 21: 957-70. pmid: 8591796.
- 761 58. Griffith LG, Swartz MA. Capturing complex 3D tissue physiology *in vitro*. *Nat Rev*
762 *Mol Cell Biol.* 2006; 7: 211-24. doi: 10.1038/nrm1858. pmid: 16496023.
- 763 59. Ma Y, Han F, Liang J, Yang J, Shi J, Xue J, et al. A species-specific activation of
764 Toll-like receptor signaling in bovine and sheep bronchial epithelial cells triggered by
765 Mycobacterial infections. *Mol Immunol.* 2016; 71: 23-33. doi:
766 10.1016/j.molimm.2016.01.004. pmid: 26802731.

- 767 60. Highlander SK. Molecular genetic analysis of virulence in *Mannheimia (Pasteurella)*
768 *haemolytica*. Front Biosci. 2001; 6: D1128-50. pmid: 11532607.
- 769 61. Frank GH, Smith PC. Prevalence of *Pasteurella haemolytica* in transported calves.
770 Am J Vet Res. 1983; 44: 981-5. pmid: 6870030.
- 771 62. Haig S-J. Adherence of *Mannheimia haemolytica* to ovine bronchial epithelial cells.
772 Biosci Horiz. 2011; 4: 50-60. doi: 10.1093/biohorizons/hzr007.
- 773 63. Clark AB, Randell SH, Nettesheim P, Gray TE, Bagnell B, Ostrowski LE. Regulation
774 of ciliated cell differentiation in cultures of rat tracheal epithelial cells. Am J Respir Cell Mol
775 Biol. 1995; 12: 329-38. doi: 10.1165/ajrcmb.12.3.7873199. pmid: 7873199.
- 776 64. Spassky N, Meunier A. The development and functions of multiciliated epithelia. Nat
777 Rev Mol Cell Biol. 2017. doi: 10.1038/nrm.2017.21. pmid: 28400610.
- 778 65. Taha-Abdelaziz K, Wyer L, Berghuis L, Bassel LL, Clark ME, Caswell JL.
779 Regulation of tracheal antimicrobial peptide gene expression in airway epithelial cells of
780 cattle. Vet Res. 2016; 47: 44. doi: 10.1186/s13567-016-0329-x.
- 781 66. Diamond G, Russell JP, Bevins CL. Inducible expression of an antibiotic peptide gene
782 in lipopolysaccharide-challenged tracheal epithelial cells. Proc Natl Acad Sci U S A. 1996;
783 93: 5156-60.
- 784 67. Mitchell GB, Al-Haddawi MH, Clark ME, Beveridge JD, Caswell JL. Effect of
785 corticosteroids and neuropeptides on the expression of defensins in bovine tracheal epithelial
786 cells. Infect Immun. 2007; 75. doi: 10.1128/IAI.00686-06.
- 787 68. Taha-Abdelaziz K, Perez-Casal J, Schott C, Hsiao J, Attah-Poku S, Slavic D, et al.
788 Bactericidal activity of tracheal antimicrobial peptide against respiratory pathogens of cattle.
789 Vet Immunol Immunopathol. 2013; 152. doi: 10.1016/j.vetimm.2012.12.016.

- 790 69. Coburn J, Frank DW. Macrophages and Epithelial Cells Respond Differently to the
791 *Pseudomonas aeruginosa* Type III Secretion System. *Infect Immun.* 1999; 67: 3151-4. pmid:
792 PMC96636.
- 793 70. Cano V, Moranta D, Llobet-Brossa E, Bengoechea JA, Garmendia J. *Klebsiella*
794 *pneumoniae* triggers a cytotoxic effect on airway epithelial cells. *BMC Microbiol.* 2009; 9:
795 156. doi: 10.1186/1471-2180-9-156. pmid: 19650888.
- 796 71. McClenahan D, Hellenbrand K, Atapattu D, Aulik N, Carlton D, Kapur A, et al.
797 Effects of Lipopolysaccharide and *Mannheimia haemolytica* Leukotoxin on Bovine Lung
798 Microvascular Endothelial Cells and Alveolar Epithelial Cells. *Clin Vaccine Immunol.* 2008;
799 15: 338-47. doi: 10.1128/CVI.00344-07. pmid: PMC2238055.
- 800 72. Kim M, Ashida H, Ogawa M, Yoshikawa Y, Mimuro H, Sasakawa C. Bacterial
801 Interactions with the Host Epithelium. *Cell Host Microbe.* 2010; 8: 20-35. doi:
802 <https://doi.org/10.1016/j.chom.2010.06.006>.
- 803 73. Ribet D, Cossart P. How bacterial pathogens colonize their hosts and invade deeper
804 tissues. *Microbes Infect.* 2015; 17: 173-83. doi: <https://doi.org/10.1016/j.micinf.2015.01.004>.
- 805 74. Bals R, Hiemstra PS. Innate immunity in the lung: how epithelial cells fight against
806 respiratory pathogens. *Eur Respir J.* 2004; 23: 327-33. doi: 10.1183/09031936.03.00098803.
807 pmid: 14979512.
- 808 75. Ganesan S, Comstock AT, Sajjan US. Barrier function of airway tract epithelium.
809 *Tissue Barriers.* 2013; 1: e24997. doi: 10.4161/tisb.24997. pmid: 24665407.
- 810 76. Plotkowski MC, de Bentzmann S, Pereira SH, Zahm JM, Bajolet-Laudinat O, Roger
811 P, et al. *Pseudomonas aeruginosa* internalization by human epithelial respiratory cells
812 depends on cell differentiation, polarity, and junctional complex integrity. *Am J Respir Cell*
813 *Mol Biol.* 1999; 20: 880-90. doi: 10.1165/ajrcmb.20.5.3408. pmid: 10226058.

814 77. Kim JY, Sajjan US, Krasan GP, LiPuma JJ. Disruption of tight junctions during
815 traversal of the respiratory epithelium by *Burkholderia cenocepacia*. *Infect Immun*. 2005; 73:
816 7107-12. doi: 10.1128/iai.73.11.7107-7112.2005. pmid: 16239504.

817 78. Higgins G, Fustero Torre C, Tyrrell J, McNally P, Harvey BJ, Urbach V. Lipoxin A4
818 prevents tight junction disruption and delays the colonization of cystic fibrosis bronchial
819 epithelial cells by *Pseudomonas aeruginosa*. *Am J Physiol Lung Cell Mol Physiol*. 2016;
820 310: L1053.

821

822 **Figure 1. Infection of undifferentiated BBEC cultures by *M. haemolytica* strains.** BBEC
823 cultures were infected apically with *M. haemolytica* strains PH2 or PH202 (2.5×10^7
824 cfu/insert) at day 0 post-ALI. At 0.5, 1, 2 and 24 hpi, cultures were apically washed to
825 remove unbound bacteria, and colonisation assessed. (A) Quantification of the number of (i)
826 adherent *M. haemolytica* and (ii) *M. haemolytica* present in the apical wash, as expressed as a
827 percentage of the original inoculum. Three inserts were analysed per time point, and the data
828 represents the mean +/- standard deviation from cultures derived from three different animals.
829 (B-C) Cultures were fixed at the stated time post-infection and immunostained to detect
830 colonisation of *M. haemolytica* with (B) β -tubulin (*M. haemolytica* - green; β -tubulin - red;
831 nuclei – blue; x1000 magnification) or (C) tight junctions (*M. haemolytica* - green; ZO-1 -
832 red; nuclei – blue; x1000 magnification). Representative images are shown of *M.*
833 *haemolytica* strains (i) PH2 or (ii) PH202 at 2 and 24 hpi (see Fig S1 and S2).

834 **Figure 2. Differentiated BBEC cultures replicate the bovine bronchial epithelium.**
835 BBEC cultures were grown for 21 days at an ALI before fixation; sample of *ex vivo* tissue
836 were also taken from the donor animal. Morphology was subsequently assessed using (A)
837 examination by SEM (x2500 magnification) and (B) H&E stained histological sections
838 (x1000 magnification). Representative images are shown of (i) *ex vivo* bovine bronchial
839 epithelium and (ii) uninfected differentiated BBECs 21 days post-ALI. (C) BBEC cultures
840 21 days post-ALI were immunostained for markers of differentiation. Representative images
841 are shown displaying (i) cilia formation (β -tubulin - red; nuclei – blue; x1000 magnification)
842 and (ii) tight junction formation (ZO-1 - red; nuclei – blue; x1000 magnification).

843 **Figure 3. Adhesion of PH2 and PH202 to differentiated BBEC cultures.** BBEC cultures
844 were infected apically with *M. haemolytica* strains PH2 or PH202 (2.5×10^7 cfu/insert) at day
845 21 post-ALI. At stated time points post-infection, cultures were apically washed to remove
846 unbound bacteria. Quantification of the number of (A) adherent *M. haemolytica* and (B) *M.*

847 *haemolytica* present in the apical wash per insert, as expressed as a percentage of the original
848 inoculum. Three inserts were analysed per time point, and the data represents the mean +/-
849 standard deviation.

850 **Figure 4. Infection of differentiated BBEC cultures by *M. haemolytica* PH2.** BBEC
851 cultures were infected apically with *M. haemolytica* strain PH2 (2.5×10^7 cfu/insert) at day 21
852 post-ALI. At stated time points post-infection, cultures were apically washed to remove
853 unbound bacteria, and fixed. Colonisation of PH2 was subsequently assessed using (A)
854 immunofluorescence labelling of PH2 and cilia (*M. haemolytica* - green; β -tubulin - red;
855 nuclei – blue; x1000 magnification), (B) examination by SEM (x2500 magnification) and (C)
856 immunohistochemical-labelling of PH2 in histological sections (OmpA-labelled *M.*
857 *haemolytica* stained brown; x1000 magnification). Representative images are shown of
858 BBEC cultures at (i) 6, (ii) 12, (iii) 16, (iv) 20 and (v) 24 hpi (see Fig S3, S4 and S5).

859 **Figure 5. Infection of differentiated BBEC cultures by *M. haemolytica* PH202.** BBEC
860 cultures were infected apically with *M. haemolytica* strain PH202 (2.5×10^7 cfu/insert) at day
861 21 post-ALI. At stated time points post-infection, cultures were apically washed to remove
862 unbound bacteria, and fixed. Colonisation of PH202 was subsequently assessed using (A)
863 immunofluorescence labelling of PH202 and cilia (*M. haemolytica* - green; β -tubulin - red;
864 nuclei – blue; x1000 magnification), (B) examination by SEM (x2500 magnification) and (C)
865 immunohistochemical-labelling of PH202 in histological sections (OmpA-labelled *M.*
866 *haemolytica* stained brown; x1000 magnification). Representative images are shown of
867 BBEC cultures at (i) 6, (ii) 12, (iii) 16, (iv) 20 and (v) 24 hpi (see Fig S3, S4 and S5).

868 **Figure 6. Histological assessment of *M. haemolytica* infection of differentiated BBEC**
869 **cultures.** BBEC cultures were infected apically with *M. haemolytica* strains (A) PH2 or (B)
870 PH202 (2.5×10^7 cfu/insert) at day 21 post-ALI. At stated time points post-infection, cultures

871 were apically washed to remove unbound bacteria, fixed and paraffin-embedded using
872 standard histological techniques. Sections were subsequently cut, deparaffinised and H&E
873 stained. Representative images are shown of BBEC cultures at (i) 6, (ii) 12, (iii) 16, (iv) 20
874 and (v) 24 hpi (x1000 magnification; see Fig S6).

875 **Figure 7. Internalisation of *M. haemolytica* in differentiated BBEC cultures.** BBEC
876 cultures were infected apically with *M. haemolytica* strains PH2 or PH202 (2.5×10^7
877 cfu/insert) at day 21 post-ALI. At 24 hpi, cultures were apically washed to remove unbound
878 bacteria. (A) The number of intracellular bacteria was quantified using a gentamicin
879 protection assay, expressed as a percentage of the original inoculum. Three inserts were
880 analysed per condition, and the data represents the mean +/- standard deviation. (B-C) BBEC
881 cultures infected with PH2 (24 hpi) were assessed using microscopy. (B) Z-stack orthogonal
882 representation of a BBEC culture labelled for PH2 and cilia (*M. haemolytica* - green; β -
883 tubulin - red; nuclei – blue; x630 magnification). (C) Examination by SEM. Representative
884 images shown of (i) invasion of a non-ciliated epithelial cell by PH2 (x10000 magnification)
885 and (ii) an epithelial cell with apical membrane removed displaying intracellular PH2 (x5000
886 magnification).

887 **Figure 8. Tight junction integrity in differentiated BBEC cultures following *M.***
888 ***haemolytica* infection.** BBEC cultures were infected apically with *M. haemolytica* strains
889 PH2 or PH202 (2.5×10^7 cfu/insert) at day 21 post-ALI. At stated time points post-infection,
890 cultures were apically washed to remove unbound bacteria. Colonisation and tight junction
891 integrity was subsequently assessed using (A) labelling of *M. haemolytica* and ZO-1 (*M.*
892 *haemolytica* - green; ZO-1 - red; nuclei – blue; x1000 magnification). Representative images
893 are shown of BBEC cultures at (i) 6, (ii) 12, (iii) 16, (iv) 20 and (v) 24 hpi (see Fig S7). (B)
894 Tight-junction integrity of BBEC cultures apically infected with *M. haemolytica* was also
895 assessed by measuring the TEER at the stated time points post-infection. (C) BBEC cultures

896 were treated for 18 h with differing concentrations of lipoxin A4 to stabilise tight junctions
897 prior to apical infection with *M. haemolytica* strain PH2 (2.5×10^7 cfu/insert) at day 21 post-
898 ALI. At 24 hpi, cultures were apically washed to remove unbound bacteria, and the number
899 of adherent *M. haemolytica* quantified and expressed as a percentage of the original
900 inoculum. For all of the above quantifications, three inserts were analysed per condition, and
901 the data represents the mean +/- standard deviation.

902 **Figure 9. Quantification of adhesion of *M. haemolytica* strains to differentiated BBEC**
903 **cultures.** BBEC cultures were infected apically with eight strains of *M. haemolytica* ($2.5 \times$
904 10^7 cfu/insert) at day 21 post-ALI. (A) At stated time points post-infection, cultures were
905 apically washed to remove unbound bacteria, and colonisation assessed. Quantification of (i)
906 the number of adherent *M. haemolytica* and (ii) *M. haemolytica* present in the apical wash, as
907 expressed as a percentage of the original inoculum. (B) Tight-junction integrity of BBEC
908 cultures apically infected with eight strains *M. haemolytica* was also assessed by measuring
909 the TEER at the stated time points post-infection. For all of the above quantifications, three
910 inserts were analysed per condition, and the data represents the mean +/- standard deviation
911 from cultures derived from three different animals (see Fig S8).

912 **Figure 10. Colonisation of *M. haemolytica* strains to differentiated BBEC cultures.**
913 BBEC cultures were infected apically with eight strains of *M. haemolytica* (2.5×10^7
914 cfu/insert) at day 21 post-ALI. At 24 hpi, cultures were apically washed to remove unbound
915 bacteria, and fixed. Colonisation of *M. haemolytica* was subsequently assessed using (A)
916 immunohistochemical-labelling of *M. haemolytica* in histological sections (OmpA-labelled
917 *M. haemolytica* stained brown; x1000 magnification) and (B) examination by SEM (x2500
918 magnification). Representative images are shown of BBEC cultures infected with (i) PH2,
919 (ii) PH376, (iii) PH202, (iv) PH210, (v) PH278, (vi) PH376, (vii) PH62 and (viii) PH346 (see
920 Fig S9, S10 and S11).

921 **Table 1. *M. haemolytica* strains utilised in this investigation.**

922 **Table 2. Assessment of damage to the differentiated BBEC cultures following PH2 and**
923 **PH202 infection.** BBEC cultures were infected apically with *M. haemolytica* strains PH2 or
924 PH202 (2.5×10^7 cfu/insert) at day 21 post-ALI. At stated time points post-infection cultures
925 were apically washed to remove unbound bacteria, fixed and paraffin-embedded using
926 standard histological techniques. Sections were subsequently cut, deparaffinised and H&E
927 stained. Semi-quantitative assessment of the extent of bacterial colonisation and epithelial
928 integrity in the histological sections was made visually. -, no sign of infection; +, low level
929 of infection, few foci of infection present; ++, moderate level of infection, foci of infection
930 common across the entirety of the culture; +++, high level of infection, infection present
931 across the majority of the culture not confined to foci, cell layer showed high levels of
932 degradation.

933 **Table 3. Assessment of damage to the differentiated BBEC cultures following *M.***
934 ***haemolytica* infection.** BBEC cultures were infected apically with eight strains of *M.*
935 *haemolytica* (2.5×10^7 cfu/insert) at day 21 post-ALI. At stated time points post-infection
936 cultures were apically washed to remove unbound bacteria, fixed and paraffin-embedded
937 using standard histological techniques. Sections were subsequently cut, deparaffinised and
938 H&E stained (see Fig S12). Semi-quantitative assessment of the extent of bacterial
939 colonisation and epithelial integrity in the histological sections was made visually. -, no sign
940 of infection; +, low level of infection, few foci of infection present; ++, moderate level of
941 infection, foci of infection common across the entirety of the culture; +++, high level of
942 infection, infection present across the majority of the culture not confined to foci, cell layer
943 showed high levels of degradation.

944

945 **Supplementary Figure 1. Immunofluorescent-labelling of *M. haemolytica* and β -tubulin**
946 **following infection of undifferentiated BBEC cultures.** BBEC cultures were infected
947 apically with *M. haemolytica* strains PH2 or PH202 (2.5×10^7 cfu/insert) at day 0 post-ALI.
948 At 0.5, 1, 2 and 24 hpi, cultures were apically washed to remove unbound bacteria, and fixed.
949 Colonisation of PH2 and PH202 was subsequently assessed using immunofluorescence
950 labelling of *M. haemolytica* and β -tubulin (*M. haemolytica* - green; β -tubulin - red; nuclei –
951 blue; x1000 magnification).

952 **Supplementary Figure 2. Immunofluorescent-labelling of *M. haemolytica* and ZO-1**
953 **following infection of undifferentiated BBEC cultures.** BBEC cultures were infected
954 apically with *M. haemolytica* strains PH2 or PH202 (2.5×10^7 cfu/insert) at day 0 post-ALI.
955 At 0.5, 1, 2 and 24 hpi, cultures were apically washed to remove unbound bacteria, and fixed.
956 Colonisation of PH2 and PH202 was subsequently assessed using immunofluorescence
957 labelling of *M. haemolytica* and tight junctions (*M. haemolytica* - green; ZO-1 - red; nuclei –
958 blue; x1000 magnification).

959 **Supplementary Figure 3. Immunofluorescent-labelling of PH2 or PH202 and β -tubulin**
960 **following infection of differentiated BBEC cultures.** BBEC cultures were infected apically
961 with *M. haemolytica* strains PH2 or PH202 (2.5×10^7 cfu/insert) at day 21 post-ALI. At
962 stated time points post-infection, cultures were apically washed to remove unbound bacteria,
963 and fixed. Colonisation of PH2 and PH202 was subsequently assessed using
964 immunofluorescence labelling of *M. haemolytica* and cilia (*M. haemolytica* - green; β -tubulin
965 - red; nuclei – blue; x1000 magnification).

966 **Supplementary Figure 4. SEM examination of PH2 or PH202 infection of differentiated**
967 **BBEC cultures.** BBEC cultures were infected apically with *M. haemolytica* strains PH2 or
968 PH202 (2.5×10^7 cfu/insert) at day 21 post-ALI. At stated time points post-infection, cultures

969 were apically washed to remove unbound bacteria, fixed and examination by SEM (x2500
970 magnification).

971 **Supplementary Figure 5. Immunohistochemical-labelling of PH2 or PH202 in**
972 **histological sections following infection of differentiated BBEC cultures.** BBEC cultures
973 were infected apically with *M. haemolytica* strains PH2 or PH202 (2.5×10^7 cfu/insert) at day
974 21 post-ALI. At stated time points post-infection, cultures were apically washed to remove
975 unbound bacteria, fixed and paraffin-embedded using standard histological techniques.
976 Sections were subsequently cut, deparaffinised and immunohistochemistry labelling of *M.*
977 *haemolytica* was performed using an anti-OmpA antibody (OmpA-labelled *M. haemolytica*
978 stained brown; x1000 magnification). For PH2 120 hpi, the tissue layer was too damaged to
979 recover following antigen retrieval.

980 **Supplementary Figure 6. H&E staining of histological sections following PH2 or PH202**
981 **infection of differentiated BBEC cultures.** BBEC cultures were infected apically with *M.*
982 *haemolytica* strains PH2 or PH202 (2.5×10^7 cfu/insert) at day 21 post-ALI. At stated time
983 points post-infection, cultures were apically washed to remove unbound bacteria, fixed and
984 paraffin-embedded using standard histological techniques. Sections were subsequently cut,
985 deparaffinised and H&E staining was performed (x1000 magnification).

986 **Supplementary Figure 7. Immunofluorescent-labelling of PH2 or PH202 and ZO-1**
987 **following infection of differentiated BBEC cultures.** BBEC cultures were infected apically
988 with *M. haemolytica* strains PH2 or PH202 (2.5×10^7 cfu/insert) at day 21 post-ALI. At
989 stated time points post-infection, cultures were apically washed to remove unbound bacteria,
990 and fixed. Colonisation of PH2 and PH202 and tight junction integrity was subsequently
991 assessed using immunofluorescence labelling of *M. haemolytica* and tight junctions (*M.*
992 *haemolytica* - green; ZO-1 - red; nuclei – blue; x1000 magnification).

993 **Supplementary Figure 8. Quantification of adhesion of *M. haemolytica* strains to**
994 **differentiated BBEC cultures.** BBEC cultures were infected apically with eight strains of
995 *M. haemolytica* (2.5×10^7 cfu/insert) at day 21 post-ALI. At 2, 24 or 72 hpi, cultures were
996 apically washed to remove unbound bacteria, and colonisation assessed. Quantification of
997 (A) the number of adherent *M. haemolytica* and (B) *M. haemolytica* present in the apical
998 wash, as expressed as a percentage of the original inoculum. Three inserts were analysed per
999 time point, and the data represents the mean +/- standard deviation.

1000 **Supplementary Figure 9. Immunohistochemical-labelling of *M. haemolytica* strains in**
1001 **histological sections following infection of differentiated BBEC cultures.** BBEC cultures
1002 were infected apically with eight strains of *M. haemolytica* (2.5×10^7 cfu/insert) at day 21
1003 post-ALI. At 2, 24 or 72 hpi, cultures were apically washed to remove unbound bacteria,
1004 fixed and paraffin-embedded using standard histological techniques. Sections were
1005 subsequently cut, deparaffinised and immunohistochemistry labelling of *M. haemolytica* was
1006 performed using an anti-OmpA antibody (OmpA-labelled *M. haemolytica* stained brown;
1007 x1000 magnification).

1008 **Supplementary Figure 10. SEM examination of differentiated BBEC culture infected**
1009 **with bovine *M. haemolytica* isolates.** BBEC cultures were infected apically with *M.*
1010 *haemolytica* strains PH2, PH376, PH202 or PH210 (2.5×10^7 cfu/insert) at day 21 post-ALI.
1011 At 2, 24 or 72 hpi, cultures were apically washed to remove unbound bacteria, fixed and
1012 examination by SEM (x2500 magnification).

1013 **Supplementary Figure 11. SEM examination of differentiated BBEC culture infected**
1014 **with ovine *M. haemolytica* isolates.** BBEC cultures were infected apically with *M.*
1015 *haemolytica* strains PH278, PH372, PH62 or PH346 (2.5×10^7 cfu/insert) at day 21 post-ALI.

1016 At 2, 24 or 72 hpi, cultures were apically washed to remove unbound bacteria, fixed and
1017 examination by SEM (x2500 magnification).

1018 **Supplementary Figure 12. H&E staining of histological sections following *M.***

1019 ***haemolytica* infection of differentiated BBEC cultures.** BBEC cultures were infected
1020 apically with eight strains of *M. haemolytica* (2.5×10^7 cfu/insert) at day 21 post-ALI. At 2,
1021 24 or 72 hpi, cultures were apically washed to remove unbound bacteria, fixed and paraffin-
1022 embedded using standard histological techniques. Sections were subsequently cut,
1023 deparaffinised and H&E staining was performed (x1000 magnification).

Figure 1

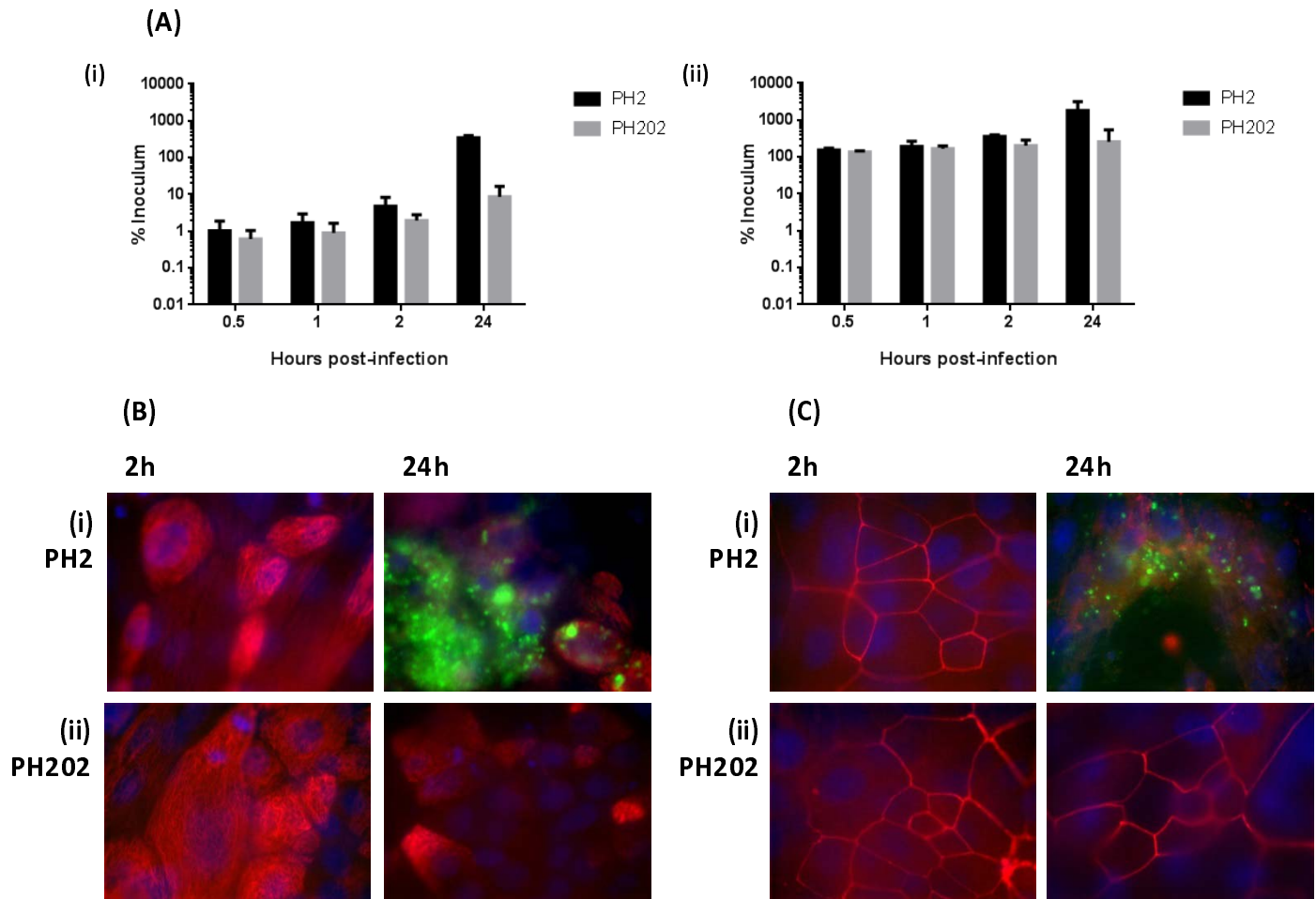


Figure 2

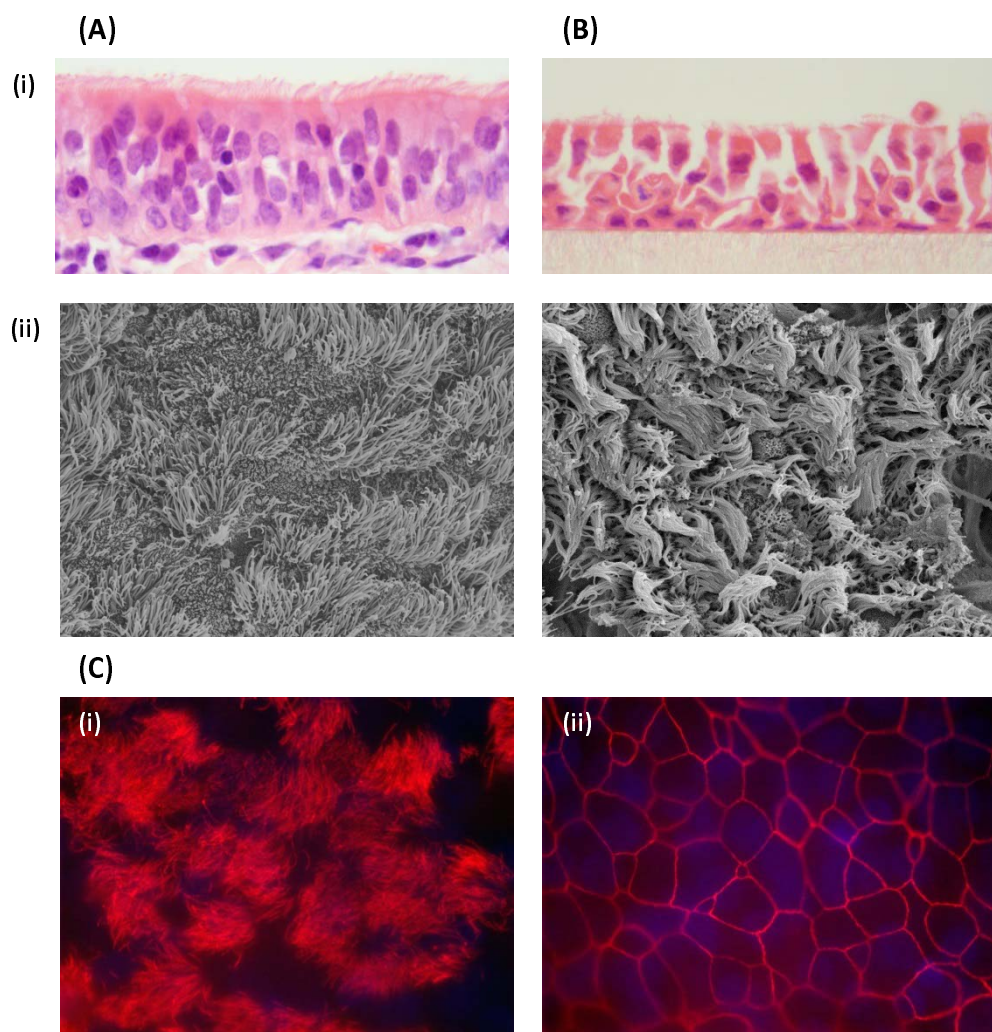


Figure 3

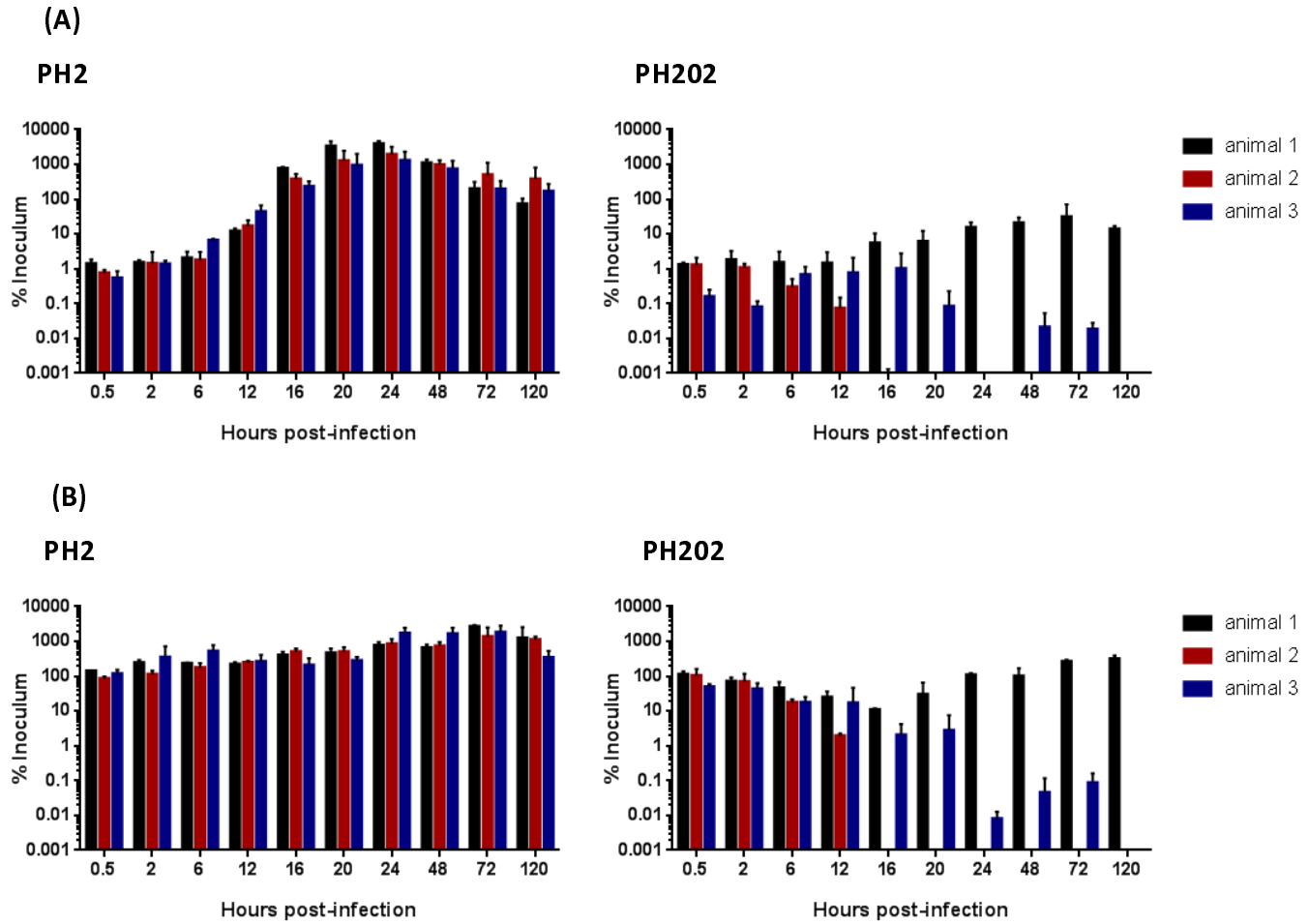


Figure 4

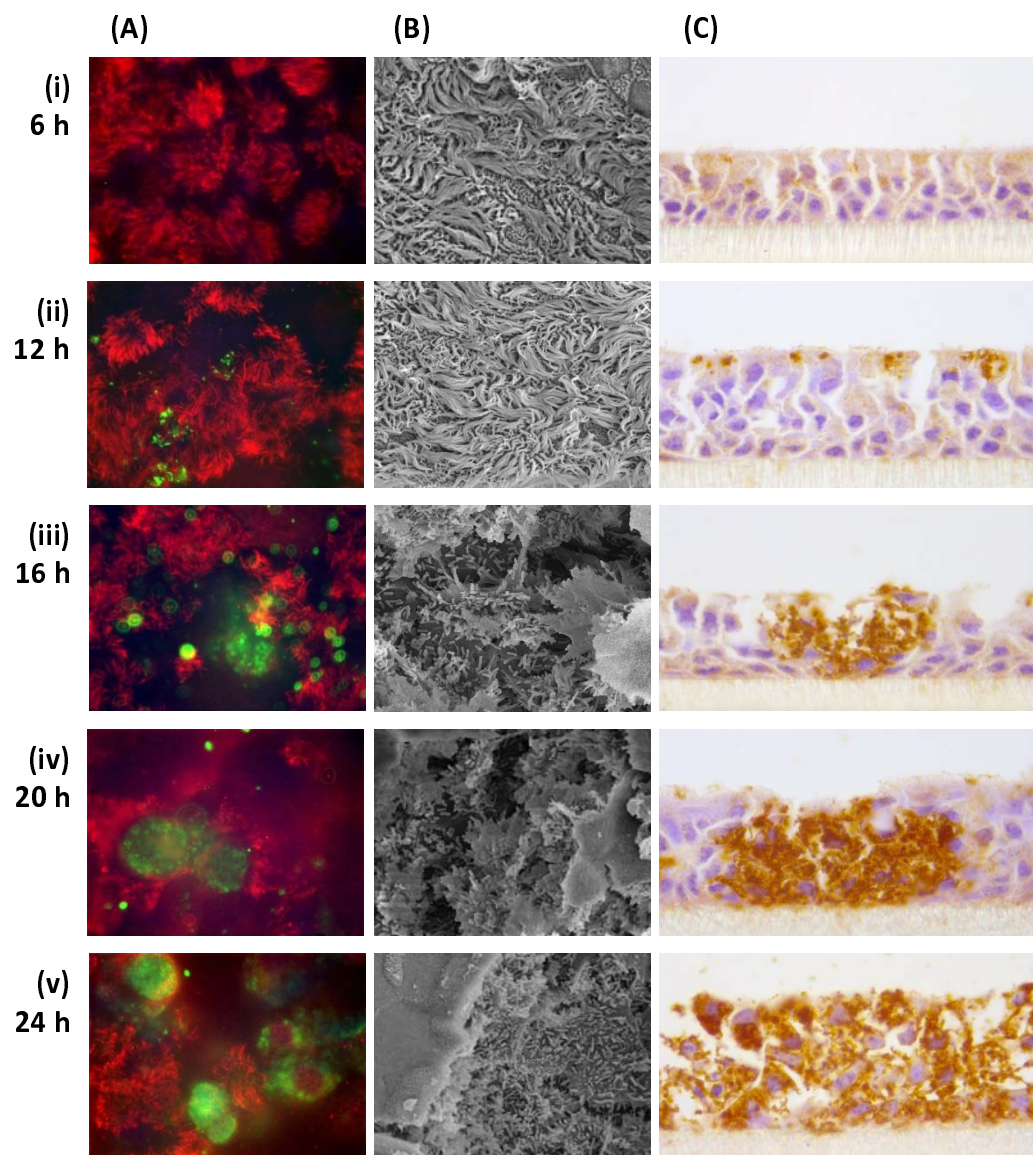


Figure 5

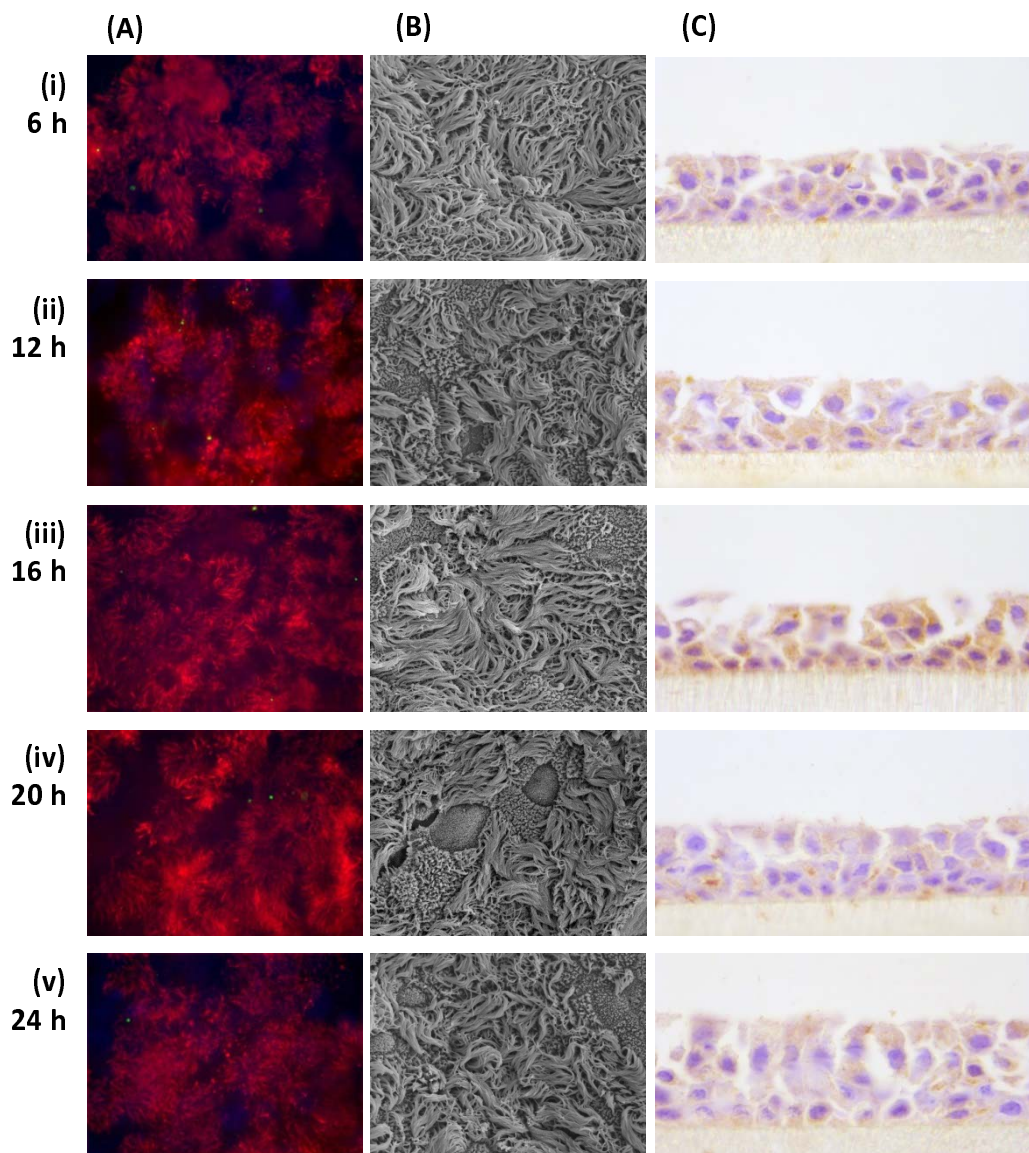


Figure 6

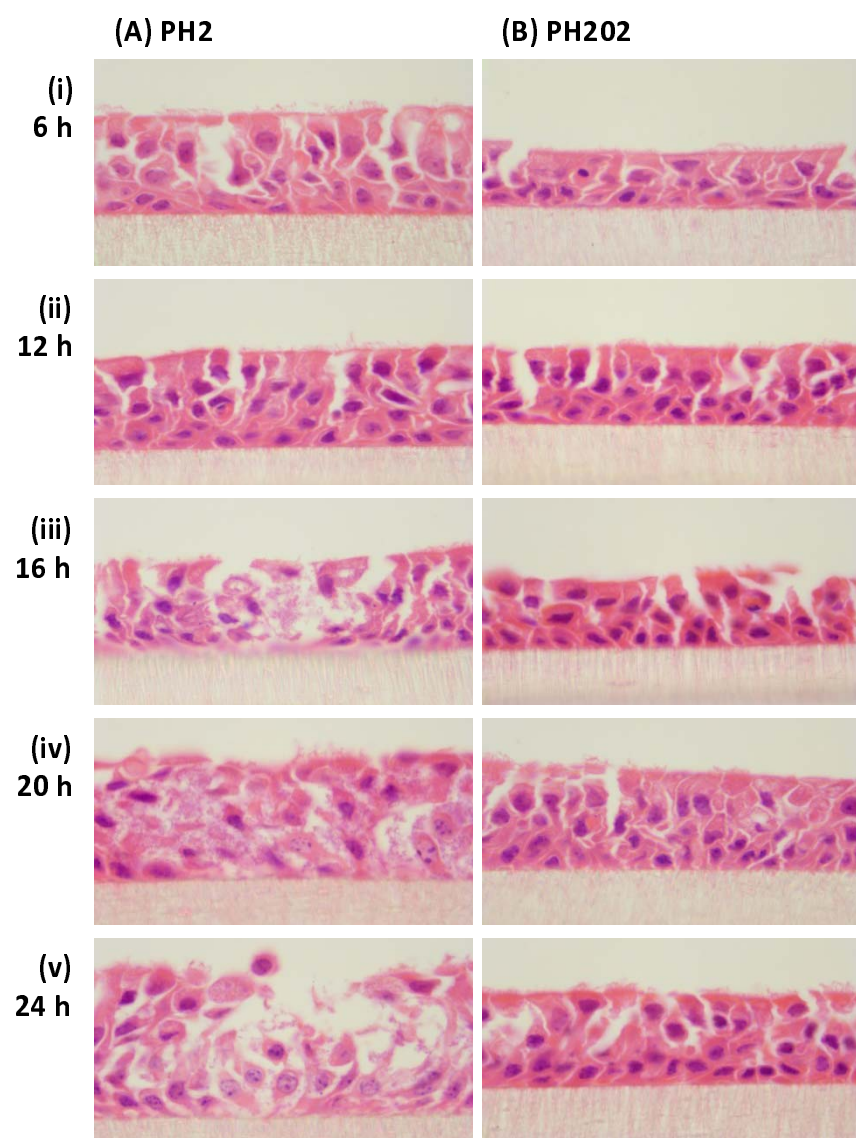


Figure 7

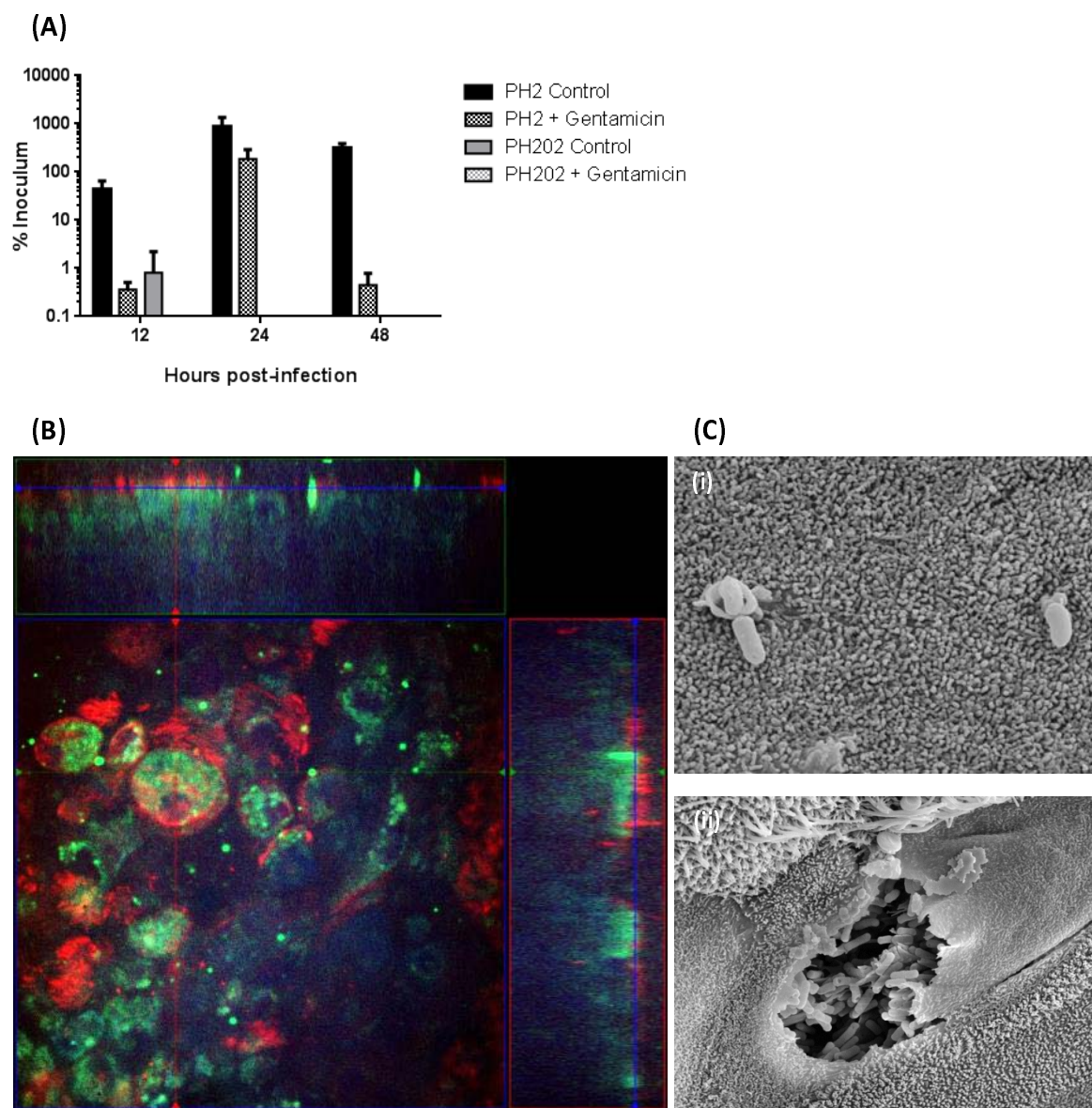


Figure 8

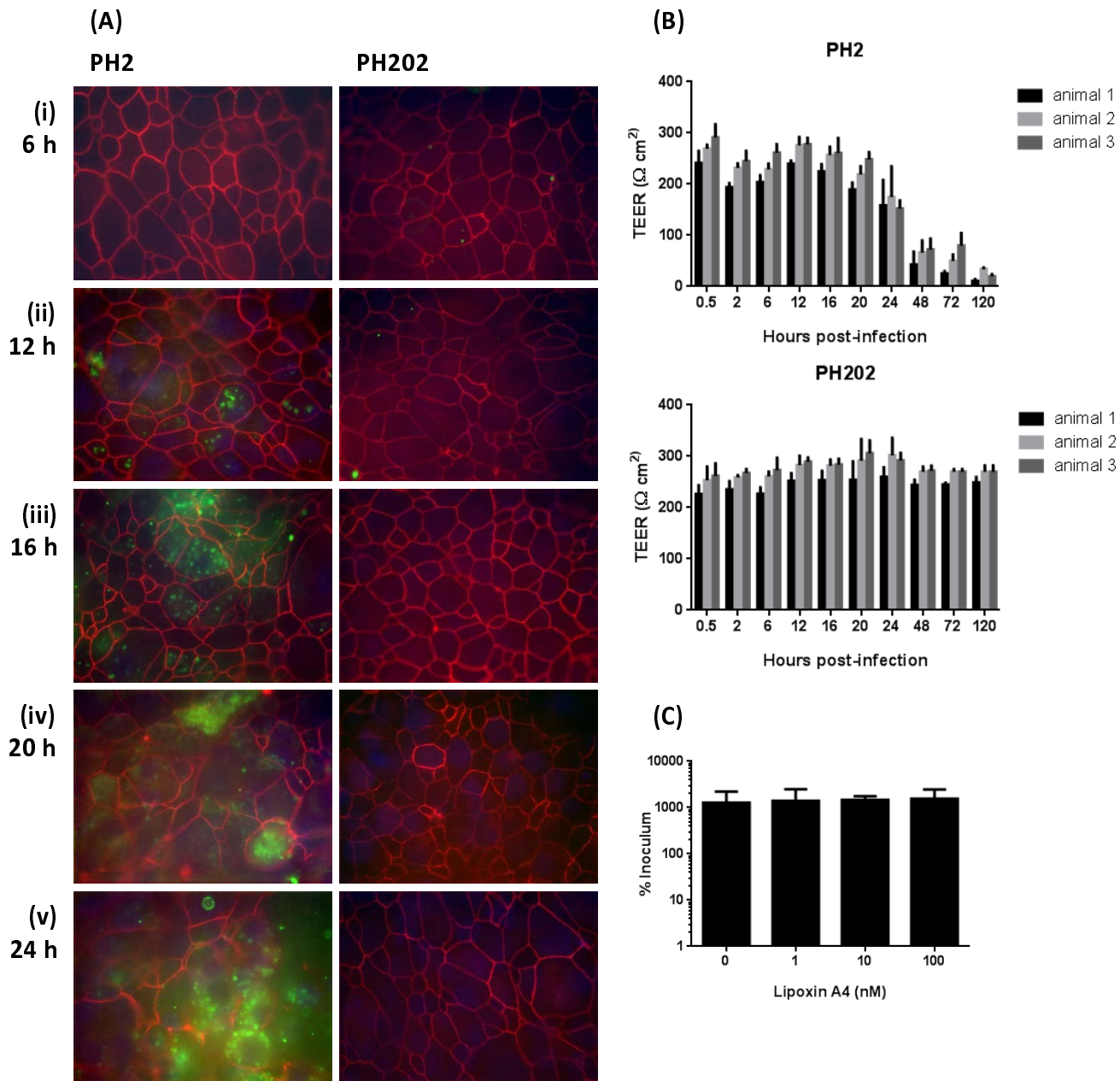


Figure 9

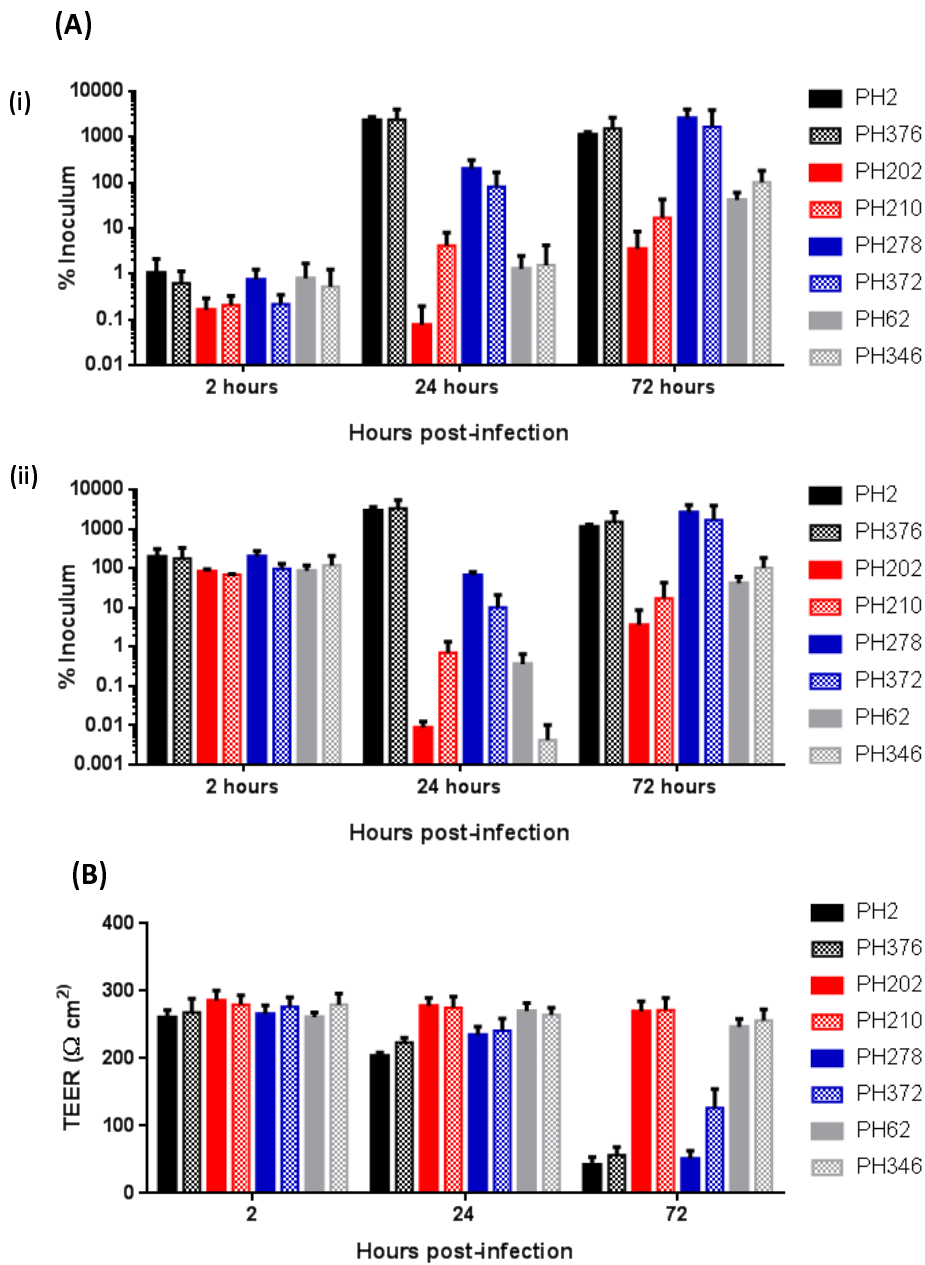


Figure 10

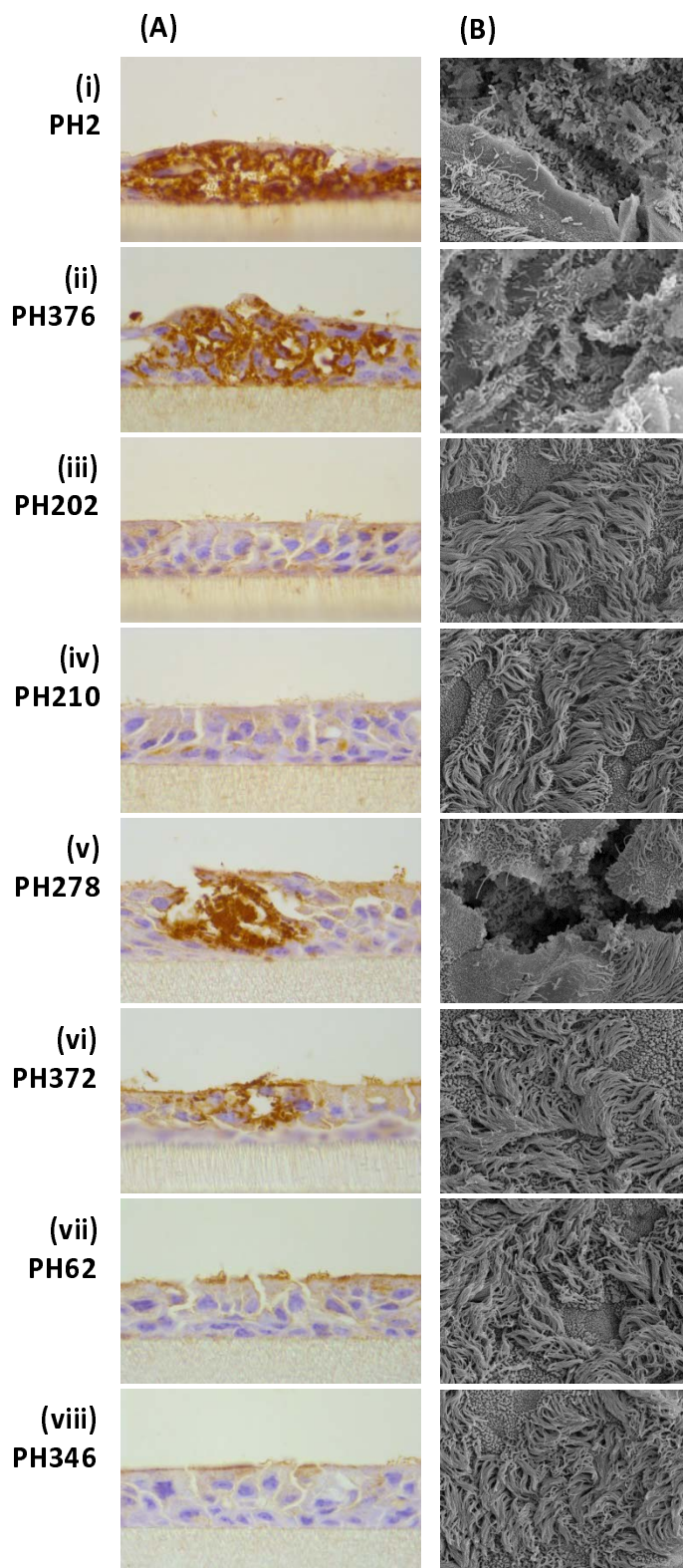


Table 1

Isolate	Serotype	Host species	Clinical status	Site of Origin
PH2	A1	Bovine	Pneumonia	Lung
PH376	A1	Bovine	Pneumonia	Lung
PH202	A2	Bovine	Healthy	Nasopharynx
PH210	A2	Bovine	Healthy	Nasopharynx
PH278	A2	Ovine	Pneumonia	Lung
PH372	A2	Ovine	Pneumonia	Lung
PH62	A12	Ovine	Healthy	Nasopharynx
PH346	A12	Ovine	Healthy	Nasopharynx

Table 2

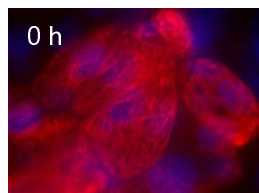
Strain	PH2			PH202		
	Animal 1	Animal 2	Animal 3	Animal 1	Animal 2	Animal 3
0.5h	-	-	-	-	-	-
2h	-	-	-	-	-	-
6h	-	-	-	-	-	-
12h	+	+	-	-	-	-
16h	++	++	++	-	-	-
20h	++	++	++	-	-	-
24h	++	++	++	-	-	-
48h	+++	+++	+++	-	-	-
72h	+++	+++	+++	-	-	-
120h	+++	+++	+++	+++	-	-

Table 3

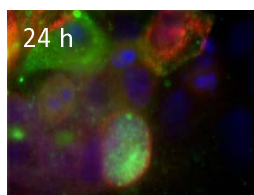
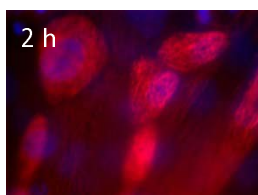
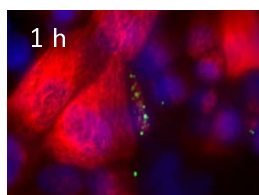
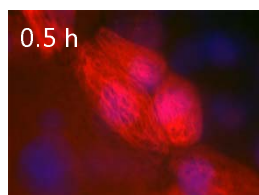
Strain	2 hours			24 hours			72 hours		
	Animal 1	Animal 2	Animal 3	Animal 1	Animal 2	Animal 3	Animal 1	Animal 2	Animal 3
PH2	-	-	-	++	++	++	+++	+++	+++
PH376	-	-	-	++	++	++	+++	+++	+++
PH202	-	-	-	-	-	-	-	-	-
PH210	-	-	-	+	-	-	-	-	-
PH278	-	-	-	++	++	+	+++	+++	++
PH372	-	-	-	+	+	+	++	+	++
PH62	-	-	-	-	+	-	+	-	-
PH346	-	-	-	+	+	-	-	-	-

Supplementary Figure 1

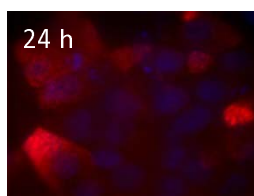
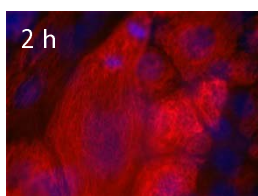
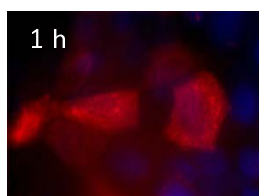
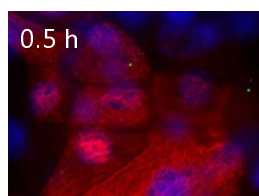
Uninfected



PH2

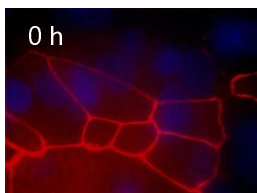


PH202

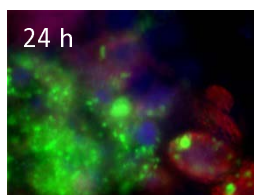
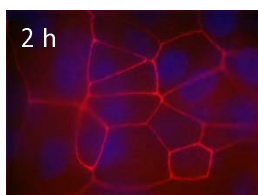
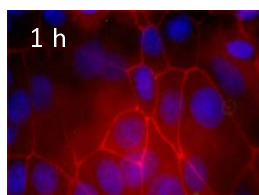
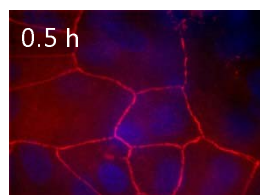


Supplementary Figure 2

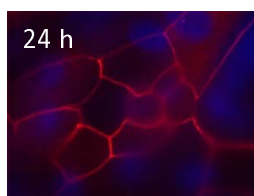
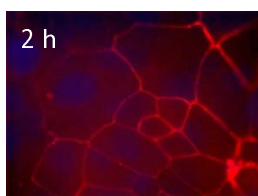
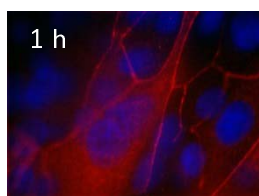
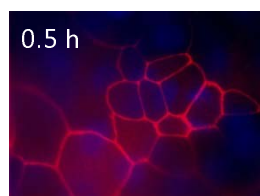
Uninfected



PH2

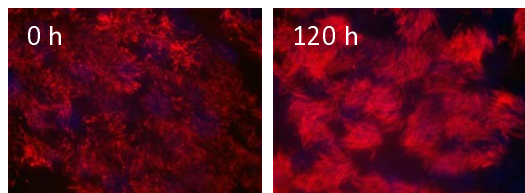


PH202

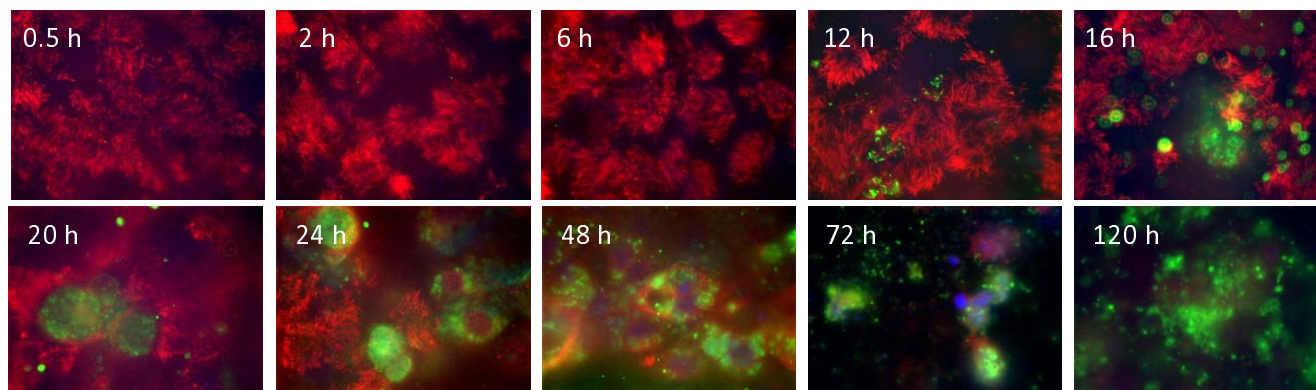


Supplementary Figure 3

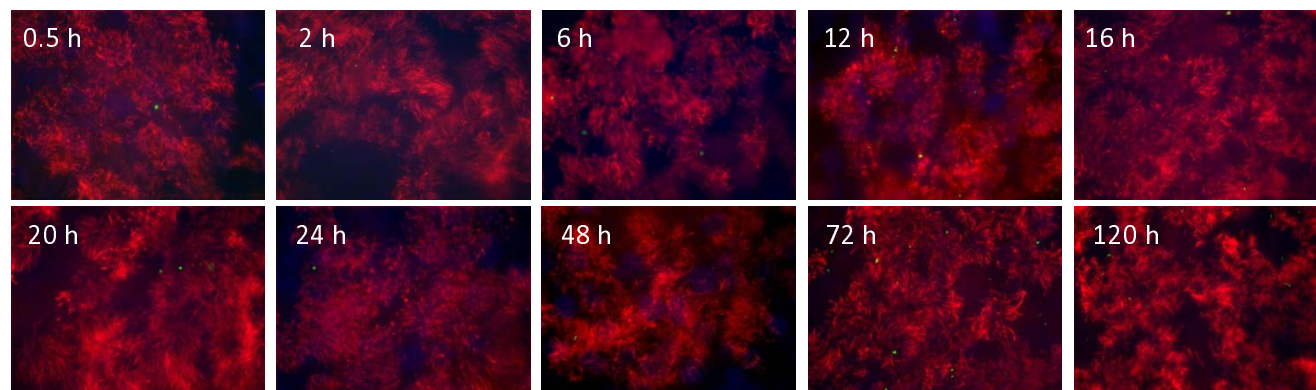
Uninfected



PH2

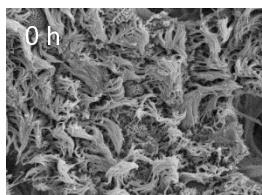


PH202

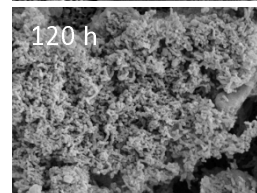
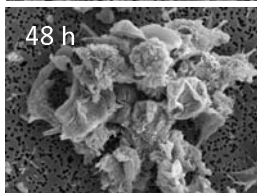
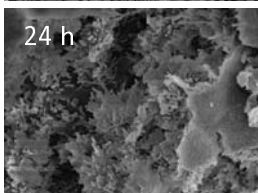
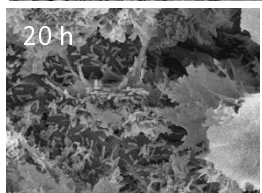
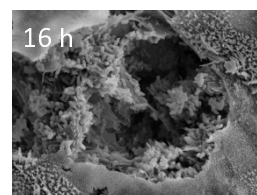
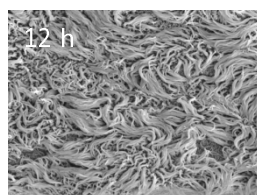
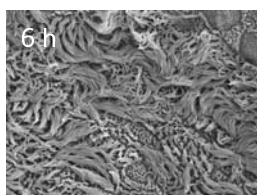
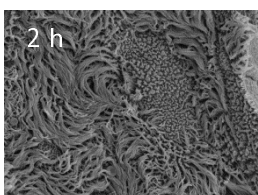
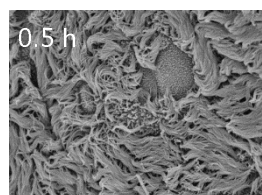


Supplementary Figure 4

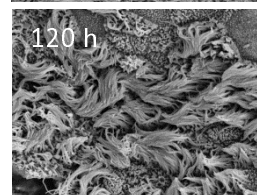
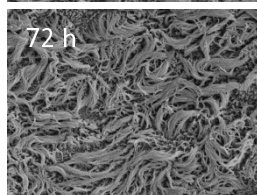
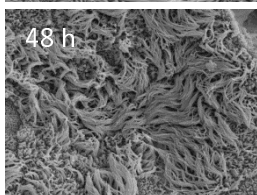
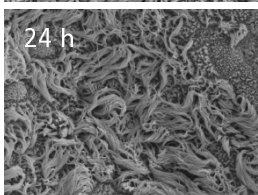
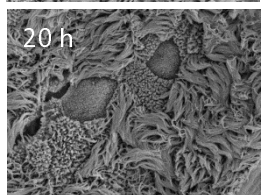
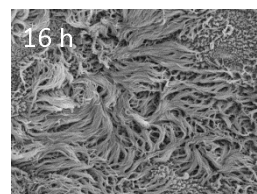
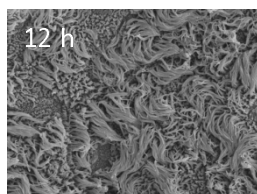
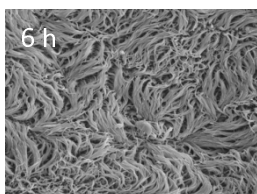
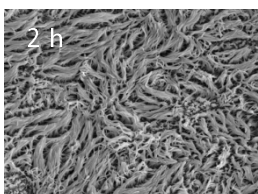
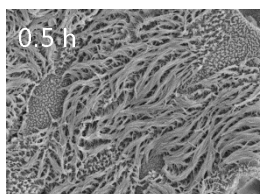
Uninfected



PH2

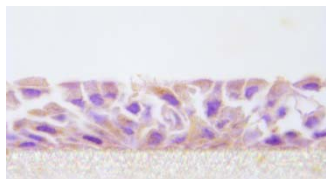


PH202

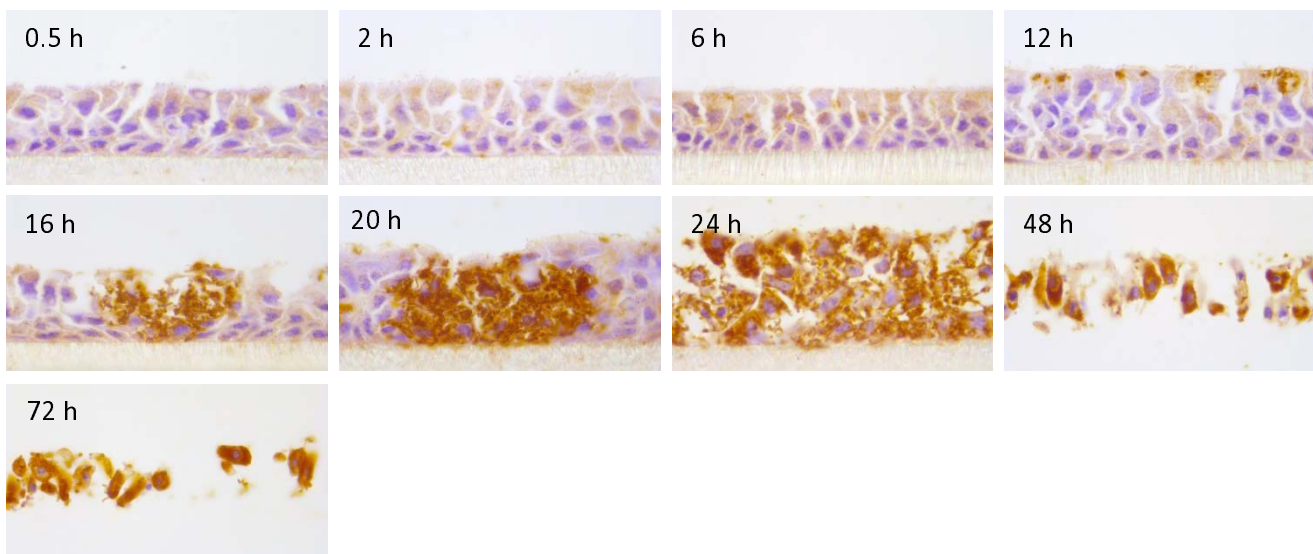


Supplementary Figure 5

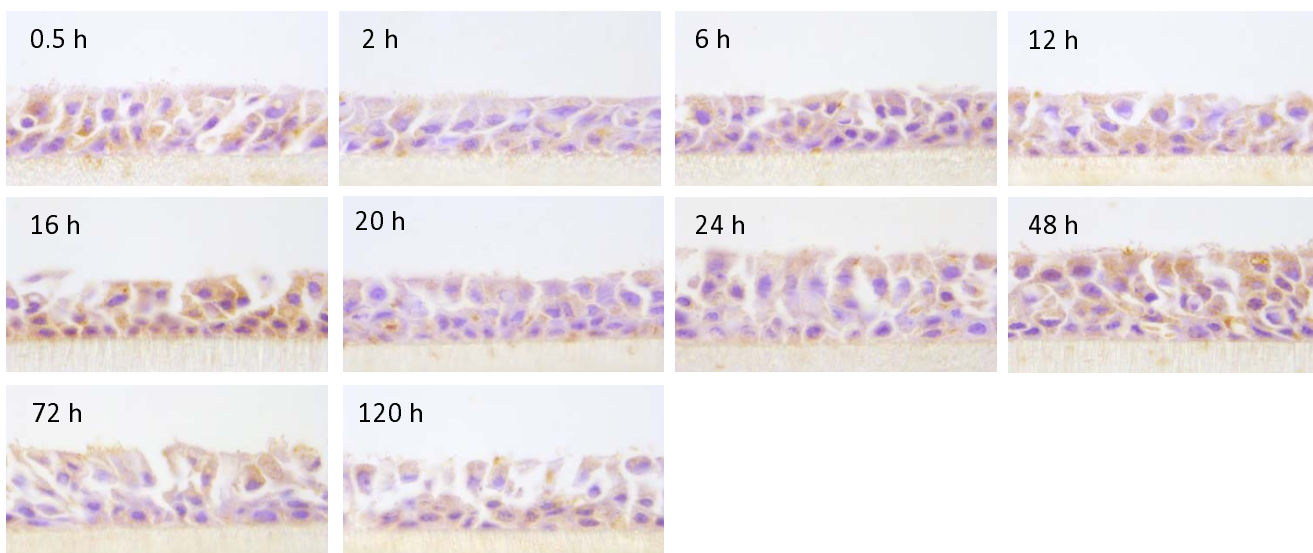
Uninfected



PH2

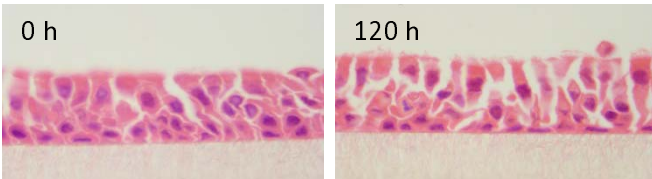


PH202

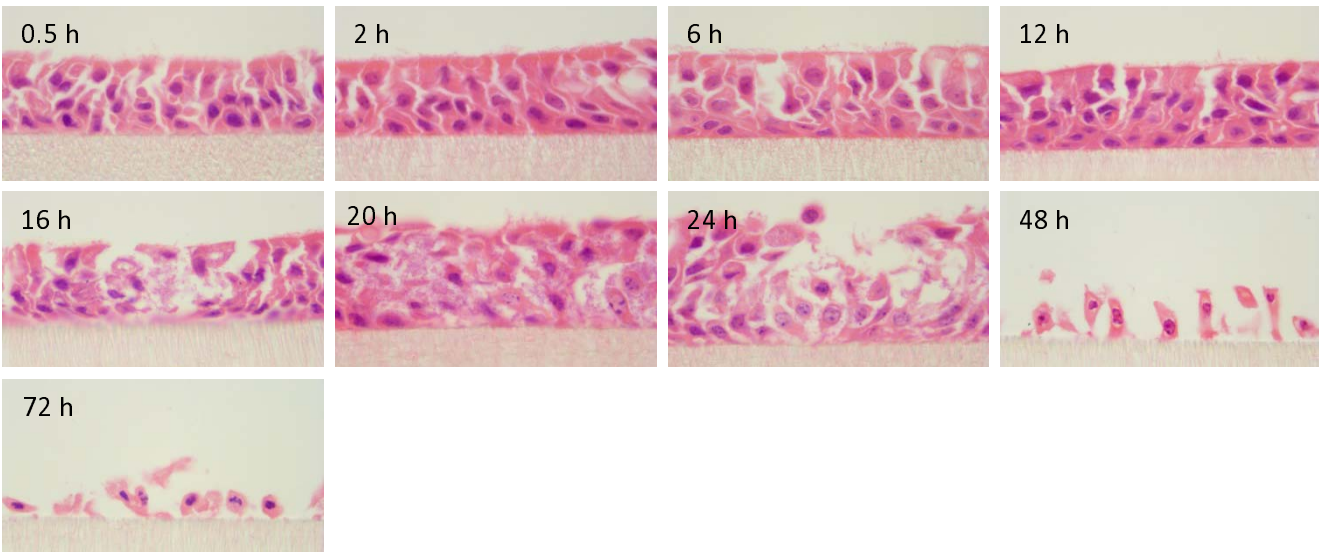


Supplementary Figure 6

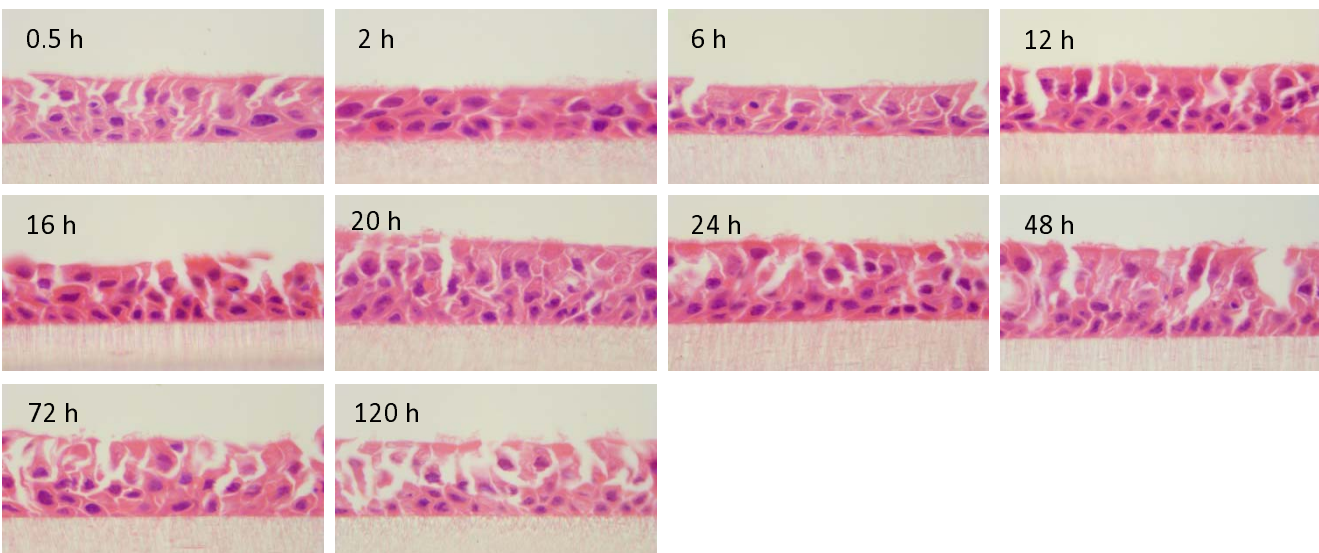
Uninfected



PH2

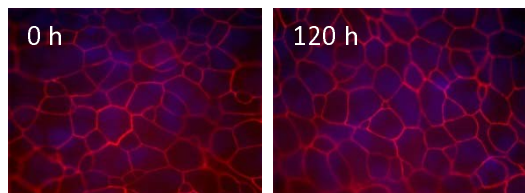


PH202

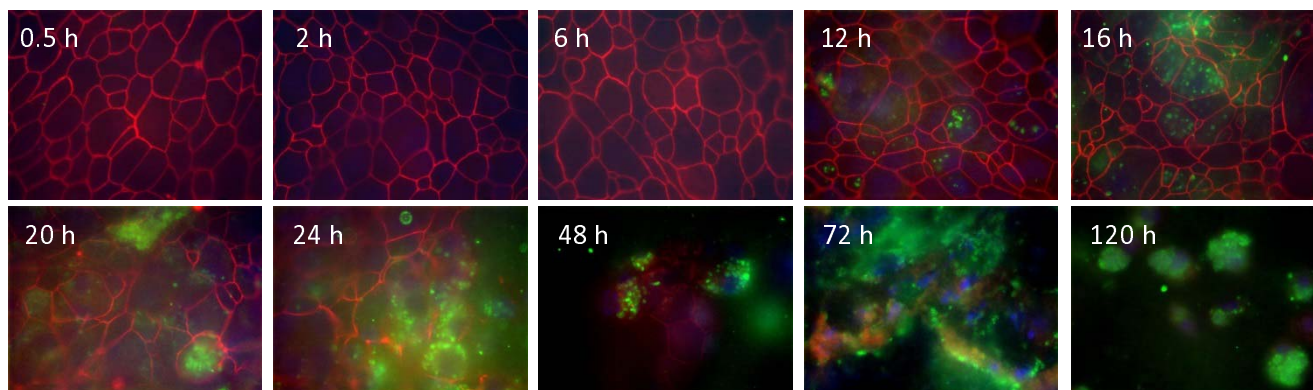


Supplementary Figure 7

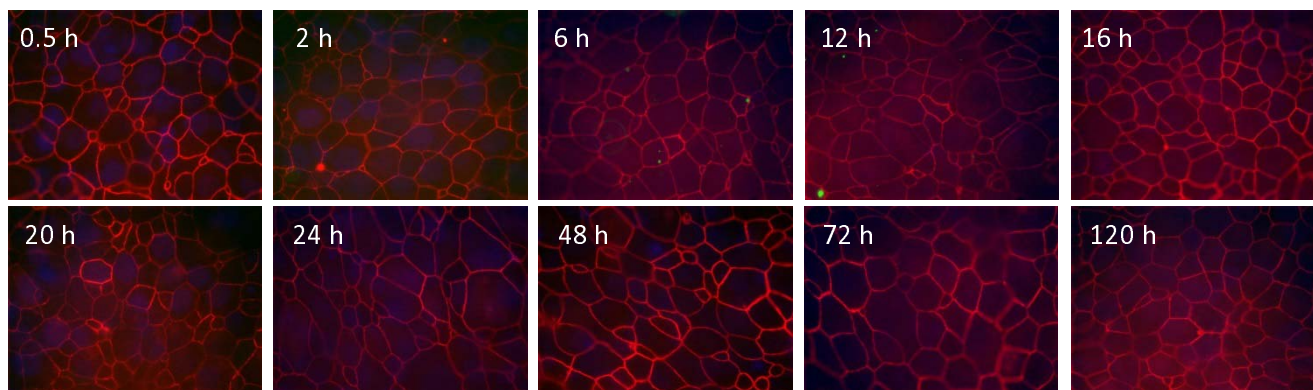
Uninfected



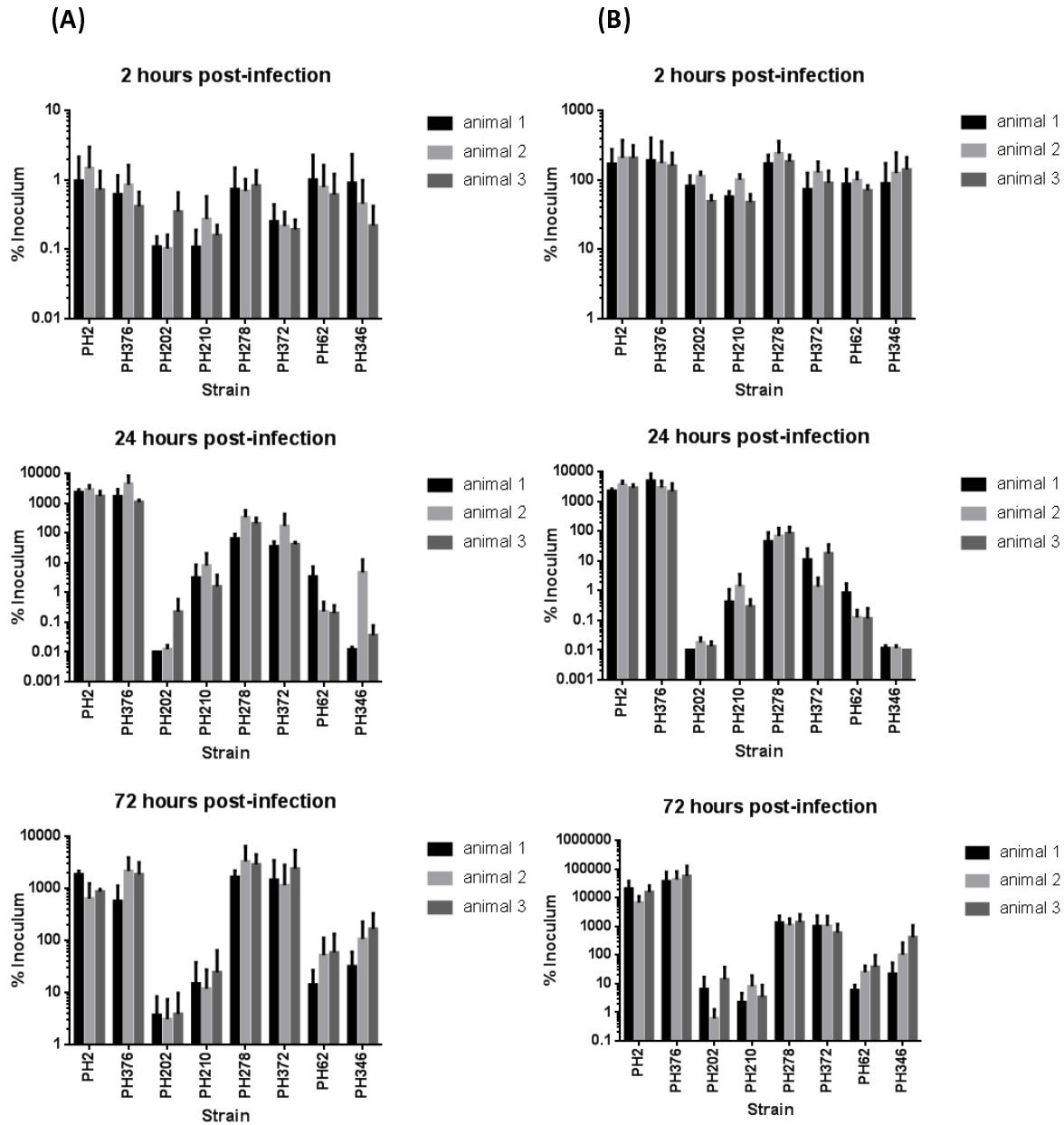
PH2



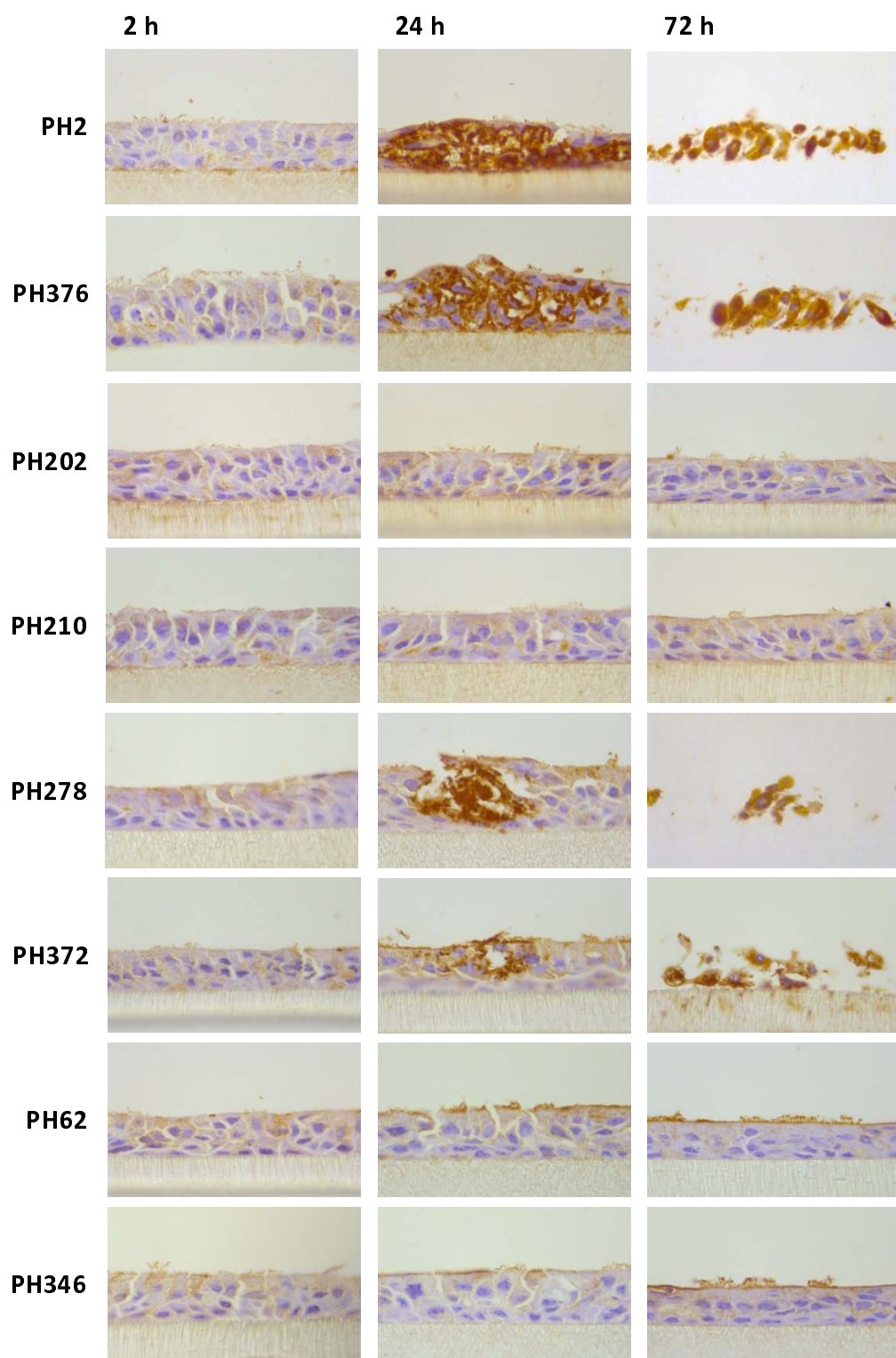
PH202



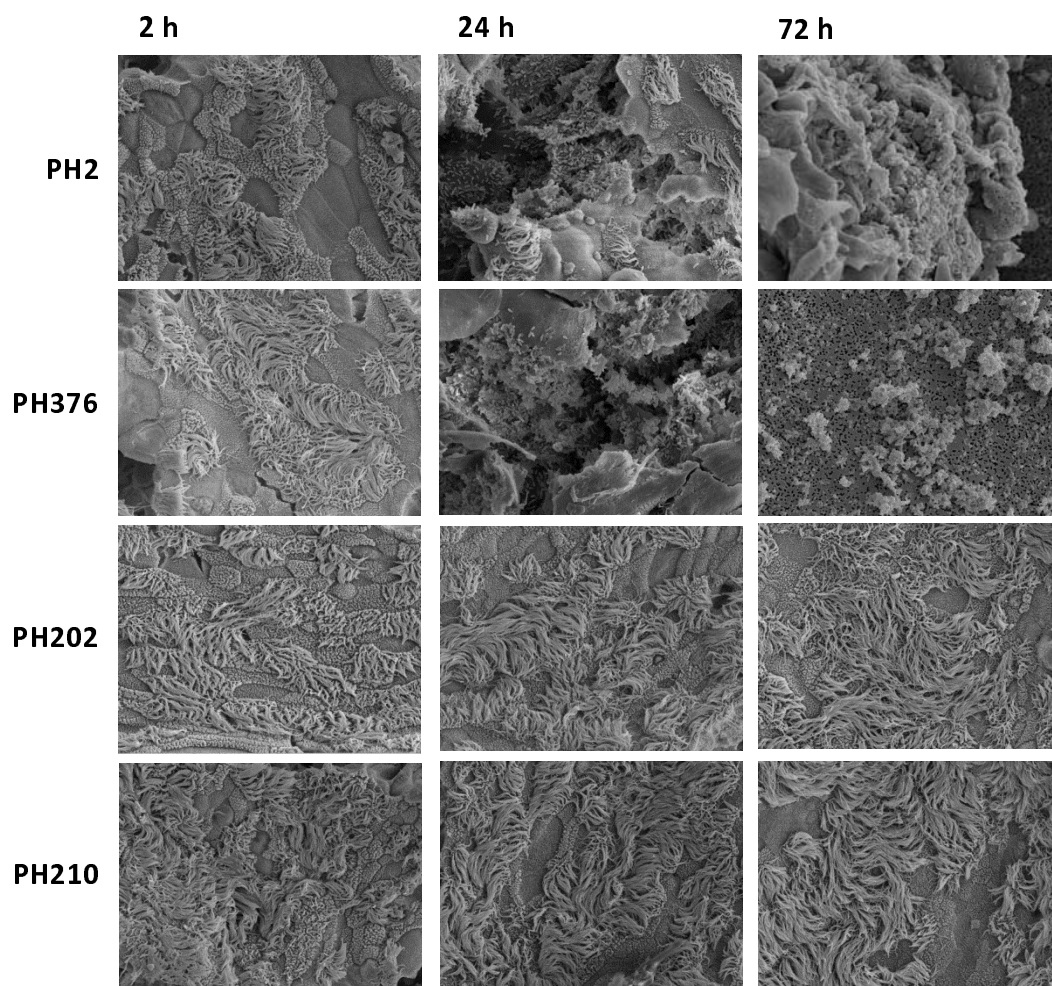
Supplementary Figure 8



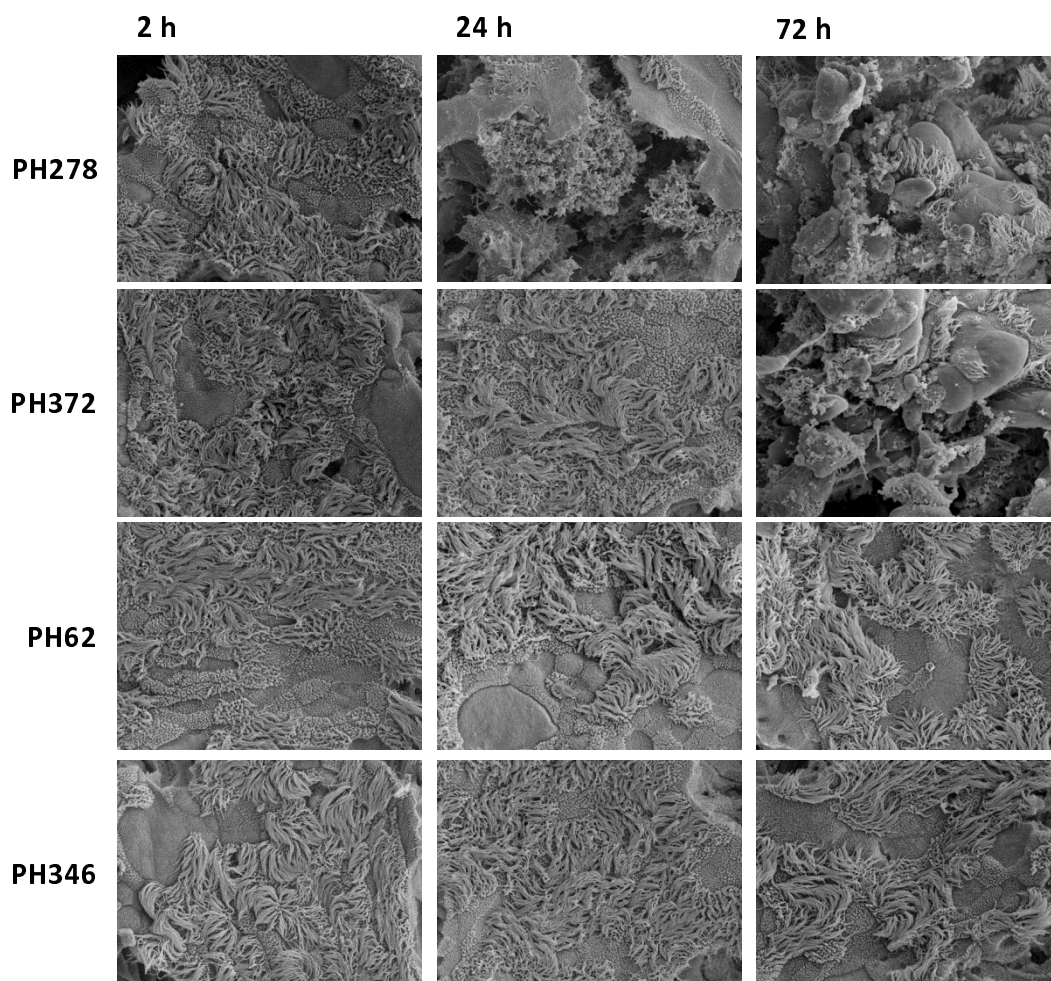
Supplementary Figure 9



Supplementary Figure 10



Supplementary Figure 11



Supplementary Figure 12

